

Oncology and Translational Medicine

Volume 3 • Number 6 • December 2017

Comparative analysis of ATP-based tumor chemosensitivity assay-directed chemotherapy versus physician-decided chemotherapy in platinum-resistant recurrent ovarian cancer
Ning Li, Yutao Gao, Wei Zhang, Xiaoguang Li, Bin Li, Haimei Tian, Yanfen Li, Lingying Wu 225

A retrospective clinical study of neoadjuvant chemotherapy for advanced epithelial ovarian cancer
Yinghui Li, Shaojia Wang, Linlin Yang, Chunmei Yin, Hongying Yang 231

Effect of parathyroid hormone on apoptosis of human medullary thyroid carcinoma cells
Xiaofeng Hou, Qinjiang Liu, Youxin Tian 241

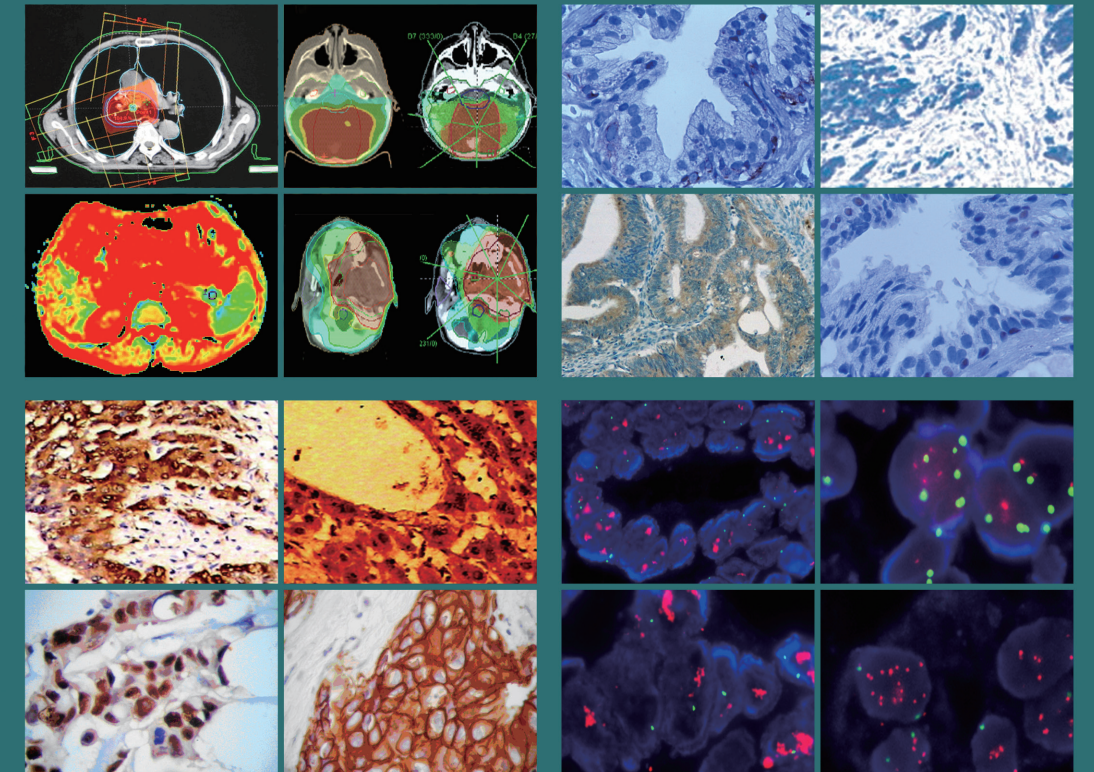
Clinical predictive values of biomarker levels in non-small cell lung cancer
Wenqing Wei 245

Function and clinical significance of SUMOylation in type I endometrial carcinoma
Xin Cui, Caixin Zhang, Yunhui Li, Yongyun Qi, Xiaoyan Ding, Shumin Hei, Weiqing Huang 249

Oncology and Translational Medicine Volume 3 • Number 6 • December 2017 pp 225-269

ISSN 2095-9621
CN 42-1865/R

Oncology and Translational Medicine



Online First
Immediately Online

otm.tjh.com.cn

Faster
publication!

邮发代号: 38-121

ISSN 2095-9621



GENERAL INFORMATION
» otm.tjh.com.cn

Volume 3
Number 6
December 2017





Honorary Editors-in-Chief

W.-W. Höpker (Germany)
Mengchao Wu (China)
Yan Sun (China)

Editors-in-Chief

Anmin Chen (China)
Shiying Yu (China)

Associate Editors

Yilong Wu (China)
Shukui Qin (China)
Xiaoping Chen (China)
Ding Ma (China)
Hanxiang An (China)
Yuan Chen (China)

Editorial Board

A. R. Hanauske (Germany)
Adolf Grünert (Germany)
Andrei Iagaru (USA)
Arnulf H. Hölscher (Germany)
Baoming Yu (China)
Bing Wang (USA)
Binghe Xu (China)
Bruce A. Chabner (USA)
Caicun Zhou (China)
Ch. Herfarth (Germany)
Changshu Ke (China)
Charles S. Cleeland (USA)
Chi-Kong Li (China)
Chris Albanese (USA)
Christof von Kalle (Germany)
D Kerr (United Kingdom)
Daoyu Hu (China)
Dean Tian (China)
Di Chen (USA)
Dian Wang (USA)
Dieter Hoelzer (Germany)
Dolores J. Schendel (Germany)
Dongfeng Tan (USA)
Dongmin Wang (China)
Ednin Hamzah (Malaysia)
Ewerbeck Volker (Germany)
Feng Li (China)
Frank Elsner (Germany)
Gang Wu (China)
Gary A. Levy (Canada)
Gen Sheng Wu (USA)
Gerhard Ehninger (Germany)
Guang Peng (USA)
Guangying Zhu (China)
Gunther Bastert (Germany)
Guoan Chen (USA)

Guojun Li (USA)
Guoliang Jiang (China)
Guoping Wang (China)
H. J. Biersack (Germany)
Helmut K. Seitz (Germany)
Hongbing Ma (China)
Hongtao Yu (USA)
Hongyang Wang (China)
Hua Lu (USA)
Huaqing Wang (China)
Hubert E. Blum (Germany)
J. R. Siewert (Germany)
Ji Wang (USA)
Jiafu Ji (China)
Jianfeng Zhou (China)
Jianjie Ma (USA)
Jianping Gong (China)
Jihong Wang (USA)
Jilin Yi (China)
Jin Li (China)
Jingyi Zhang (Canada)
Jingzhi Ma (China)
Jinyi Lang (China)
Joachim W. Dudenhausen (Germany)
Joe Y. Chang (USA)
Jörg-Walter Bartsch (Germany)
Jörg F. Debatin (Germany)
JP Armand (France)
Jun Ma (China)
Karl-Walter Jauch (Germany)
Katherine A. Siminovitch (Canada)
Kongming Wu (China)
Lei Li (USA)
Lei Zheng (USA)
Li Zhang (China)
Lichun Lu (USA)
Lili Tang (China)
Lin Shen (China)
Lin Zhang (China)
Lingying Wu (China)
Luhua Wang (China)
Marco Antonio Velasco-Velázquez (Mexico)
Markus W. Büchler (Germany)
Martin J. Murphy, Jr (USA)
Mathew Casimiro (USA)
Matthias W. Beckmann (Germany)
Meilin Liao (China)
Michael Buchfelder (Germany)
Norbert Arnold (Germany)
Peter Neumeister (Austria)
Qing Zhong (USA)
Qinghua Zhou (China)

Qingyi Wei (USA)
Qun Hu (China)
Reg Gorczynski (Canada)
Renyi Qin (China)
Richard Fielding (China)
Rongcheng Luo (China)
Shenjiang Li (China)
Shenqiu Li (China)
Shimosaka (Japan)
Shixuan Wang (China)
Shun Lu (China)
Sridhar Mani (USA)
Ting Lei (China)
Ulrich Sure (Germany)
Ulrich T. Hopt (Germany)
Ursula E. Seidler (Germany)
Uwe Kraeuter (Germany)
W. Hohenberger (Germany)
Wei Hu (USA)
Wei Liu (China)
Wei Wang (China)
Weijian Feng (China)
Weiping Zou (USA)
Wenzhen Zhu (China)
Xianglin Yuan (China)
Xiaodong Xie (China)
Xiaohua Zhu (China)
Xiaohui Niu (China)
Xiaolong Fu (China)
Xiaoyuan Zhang (USA)
Xiaoyuan (Shawn) Chen (USA)
Xichun Hu (China)
Ximing Xu (China)
Xin Shelley Wang (USA)
Xishan Hao (China)
Xiuyi Zhi (China)
Ying Cheng (China)
Ying Yuan (China)
Yixin Zeng (China)
Yongjian Xu (China)
You Lu (China)
Youbin Deng (China)
Yuankai Shi (China)
Yuguang He (USA)
Yuke Tian (China)
Yunfeng Zhou (China)
Yunyi Liu (China)
Yuquan Wei (China)
Zaide Wu (China)
Zefei Jiang (China)
Zhangqun Ye (China)
Zhishui Chen (China)
Zhongxing Liao (USA)

Oncology and Translational Medicine

December 2017 Volume 3 Number 6

Contents

Comparative analysis of ATP-based tumor chemosensitivity assay-directed chemotherapy versus physician-decided chemotherapy in platinum-resistant recurrent ovarian cancer

Ning Li, Yutao Gao, Wei Zhang, Xiaoguang Li, Bin Li, Haimei Tian, Yanfen Li, Lingying Wu 225

A retrospective clinical study of neoadjuvant chemotherapy for advanced epithelial ovarian cancer

Yinghui Li, Shaojia Wang, Linlin Yang, Chunmei Yin, Hongying Yang 231

Effect of parathyroid hormone on apoptosis of human medullary thyroid carcinoma cells

Xiaofeng Hou, Qinjiang Liu, Youxin Tian 241

Clinical predictive values of biomarker levels in non-small cell lung cancer

Wenqing Wei 245

Function and clinical significance of SUMOylation in type I endometrial carcinoma

Xin Cui, Caixin Zhang, Yunhui Li, Yongyun Qi, Xiaoyan Ding, Shumin Hei, Weiqing Huang 249

Expression of CXCL12-CXCR4 in osteosarcoma and its correlation with angiogenesis

Lu Han, Yangyang Shen, Wenhua Zhao, Baoyong Sun, Xin Zhang, Kai Cui, Lei Zhou, Sheng Li 254

A comparative study between flattening filter-free beams and flattening filter beams in radiotherapy treatment

Ali Wagdy, Khaled El Shahat, Huda Ashry, Amaal El Shershaby, Ehab Abdo 260

Primary urachal adenocarcinoma: a rare case report

Kaihua Liu, Hongqiang Wang, Lei Yu, Peitao Wang, Zhijun Liu, Lijiang Sun, Hongsheng Yu, Shenqian Li 267

Comparative analysis of ATP-based tumor chemosensitivity assay-directed chemotherapy versus physician-decided chemotherapy in platinum-resistant recurrent ovarian cancer*

Ning Li¹, Yutao Gao¹, Wei Zhang², Xiaoguang Li¹, Bin Li¹, Haimei Tian², Yanfen Li², Lingying Wu¹ (✉)

¹ Department of Gynecological Oncology, National Cancer Center/Cancer Hospital, Chinese Academy of Medical Sciences and Peking Union Medical College, Beijing 100021, China

² Biological Testing Center, National Cancer Center/Cancer Hospital, Chinese Academy of Medical Sciences and Peking Union Medical College, Beijing 100021, China

Abstract

Objective The aim of the study was to evaluate the role of ATP-based tumor chemosensitivity assay (ATP-TCA) in patients with platinum-resistant recurrent ovarian cancer (PRROC).

Methods A total of 43 patients with PRROC who underwent chemotherapy based on the results of ATP-TCA in the Cancer Hospital, Chinese Academy of Medical Sciences were included in the present study. As controls, we selected another 43 patients with PRROC who were treated at the physician's discretion within the same time period and had the same clinical characteristics as the patients in the ATP-TCA group. Log-rank test and Cox proportional hazards model were adopted for analysis.

Results A total of 86 patients were retrospectively analyzed in the present study. Patients were routinely monitored to evaluate the rate of progression-free survival (PFS). The median follow-up time was 13 months. The PFS for the ATP-TCA and control groups was 5 and 3 months, respectively ($P = 0.027$). Multivariate analysis showed that the type of treatment was an independent prognostic factor for PFS ($P = 0.040$; HR: 0.623; 95% CI: 0.313–0.973). Subgroup analysis showed that among patients with a treatment-free interval (TFI) of ≥ 3 months ($n = 50$), those in the ATP-TCA group had longer PFS than those in the control group (7 vs 4 months, $P = 0.010$). Meanwhile, the median PFS of patients who underwent ≤ 2 prior chemotherapy regimens (PCR, $n = 52$) in the ATP-TCA and control groups was 6 months and 4 months, respectively ($P = 0.025$).

Conclusion ATP-TCA-directed chemotherapy might improve the PFS in PRROC. In particular, the survival benefit from ATP-TCA is higher in patients with a TFI of ≥ 3 months or treated with ≤ 2 PCR.

Key words: epithelial ovarian cancer; platinum-resistance; recurrence; ATP-based tumor chemosensitivity assay (ATP-TCA)

Received: 2 October 2017
Revised: 3 November 2017
Accepted: 7 December 2017

The prognosis of epithelial ovarian cancer is rather poor. The 5-year survival rate for patients with advanced ovarian cancer remains at approximately 30%–40%, and chemoresistance after relapse is among the main causes. Currently, second-line chemotherapy for patients with platinum-resistant recurrent ovarian cancer (PRROC) is selected mainly based on the clinical experience of the physicians, results of clinical trials, and guidelines

from related international organizations. Several cytotoxic agents for patients with PRROC are available, including docetaxel, topotecan, gemcitabine (GEM), liposomal doxorubicin, paclitaxel (weekly therapy), and etoposide (oral). Previous reports have shown that the overall response rate of second-line chemotherapy is approximately 20%–30% [1–3]. Patients who show no response to certain chemotherapeutics might respond to

✉ Correspondence to: Lingying Wu. Email: wulingying@csc.org.cn

* Supported by a grant from the Capital's Funds for Health Improvement and Research (No. Z131107002213013).

© 2017 Huazhong University of Science and Technology

another, suggesting considerable clinical heterogeneity in tumor chemosensitivity. According to literature, a portion of patients still achieve complete remission after receiving second-line chemotherapy and has prolonged progression-free survival (PFS) of more than 5 years [3-5]. However, how to select the most effective cytotoxic drugs or drug combinations for individualized treatment remains to be solved.

A chemosensitivity assay assesses tumor responses to a particular chemotherapeutic agent by using cells primarily cultured from the tumor specimen. This allows for the identification of agents with a strong anti-tumor activity, and those with no anti-tumor activity are excluded. The result of a chemosensitivity assay provides the basis for clinical decision-making concerning chemotherapeutic regimens. Both the American Society of Clinical Oncology [6] and National Comprehensive Cancer Network [7] encourage researchers to conduct clinical trials related to chemosensitivity assay.

Several types of chemosensitivity assays have been reported. The ATP-based tumor chemosensitivity assay (ATP-TCA) was developed based on the principle that the amount of endogenous ATP in cells instantly reflects cell viability and the number of viable cells. Therefore, intracellular ATP content can be used to evaluate the anti-tumor effect of various chemotherapy drugs. In 1988, Sevin *et al* [8] at the University of Miami employed ATP-TCA for the first time to examine the chemosensitivity of ovarian cancer tissues. Since then, many studies have indicated a good correlation between the results of ATP-TCA and clinical responses in patients with ovarian cancer. However, the results of ATP-TCA were not completely consistent with the clinical response of patients with ovarian cancer in different study populations. This indicates that ATP-TCA might play a role in only a particular group of patients. A series of studies reported that chemosensitivity testing on primary ovarian cancer prior to the initial chemotherapy failed to improve the PFS and overall survival (OS) [9-12]. Initial paclitaxel (PTX)/platinum chemotherapy usually achieves a response rate of over 70% in epithelial ovarian cancer. It is highly likely that conducting ATP-TCA would not challenge the primary care for additional therapeutic benefit. Therefore, identifying patients who can benefit from ATP-TCA is important. Our previous retrospective study has shown that patients with PRROC benefit limitedly from experience-guided chemotherapy [13]. By contrast, ATP-TCA-guided chemotherapy extended PFS by 3 months (ATP-TCA guided group vs. experience-based group: 5 months vs. 2 months, respectively) [13]. Based on our previous findings, the present study further evaluated the role of ATP-TCA in the treatment of PRROC and aimed to identify the patient population who require ATP-TCA.

Materials and methods

Patients' eligibility

Patients with ROC who were admitted to Cancer Hospital, Chinese Academy of Medical Sciences between July 2010 and June 2013 were included in the present study, if the following inclusion criteria were met: (1) patients were previously histologically diagnosed with epithelial ovarian cancer; (2) patients had PRROC (the last chemotherapy was a platinum-containing regimen, and the time interval from completion of the last chemotherapy to progression or recurrence was ≤ 6 months); (3) tumor specimens or aspirates from malignant ascites/pleural effusion could be obtained for ATP-TCA; (4) patients had a Karnofsky performance status score of 60-100 points; and (5) the expected survival was more than 4 months.

Forty-three patients with PRROC were assigned to the ATP-TCA-guided chemotherapy group. This study was approved by the Cancer Hospital, Chinese Academy of Medical Sciences Institutional Review Board. All patients signed a written informed consent form. To decrease the bias from other clinical factors, we selected another 43 patients with PRROC who were treated based on the physician's discretion within the same time period and had similar clinical characteristics such as age, tumor stage, histology, grade, number of prior chemotherapy regimens (PCR) and cycles, treatment-free interval (TFI), and residual disease (if patients underwent secondary cytoreductive surgery) to the patients in ATP-TCA group as controls. TFI was calculated as the time interval from the last chemotherapy to recurrence before study enrollment. The TFI of the patients who progressed during the last chemotherapy was considered as 0.

ATP-TCA method

Tissue/cells for ATP-TCA were obtained either during the operation or from malignant effusions. Within 30 minutes, the samples were sent to the Biological Testing Center of our hospital where the ATP-TCA was conducted. The rest of the tumor tissue or abdominal/pleural effusion samples were collected for routine pathological and cytological examinations.

Detection reagents, instruments, and methods

The detection kit was purchased from Jin Zijing Biomedical Technology Co., Ltd (Beijing, China). The fluorescence scanner was purchased from Hamamatsu Photonics Co., Ltd (Beijing, China). The experimental procedure was conducted in strict accordance with the manufacturer's instructions. All tests were completed at the Biological Testing Center of our hospital. Briefly, cells were dissociated from solid tumor samples via enzymatic digestion overnight and purified via density

centrifugation. Density centrifugation was also used to obtain cells from ascites/pleural effusion aspirate. The cells were resuspended in a complete assay medium and were then plated at 20 000 cells/well in polypropylene 96-well plates. In general, sufficient ovarian cancer cells were available for testing 14 different drugs or drug combinations at 6 concentrations. Triplicate wells were set up for each drug dose, ranging from 6.25% to 200% of peak plasma concentrations (PPC) for each drug or drug combination. At the end of a 5-day incubation period, the ATP content of the cells was measured using the luciferin-luciferase assay. Results were deemed evaluable if the following criteria were fulfilled:

(1) Histological and/or cytological diagnosis of ovarian carcinoma on the assay specimen with > 20% malignant cells; (2) No inhibition medium. Only control value > 20 nmol/L ATP and maximum inhibitor control \leq 1% of medium; (3) Concentration responsiveness to agents previously shown to exhibit such responsiveness in the assay; and (4) Absence of fungal or bacterial contamination.

Evaluation criteria for the ATP-TCA results

The results of the ATP-TCA were evaluated using the sensitivity index (SI) method. SI was calculated according to the following formula: $SI = 600 - \Sigma(\text{tumor growth inhibition rates at 6 drug concentrations})$. The 6 concentrations utilized in the present study were 200%, 100%, 50%, 25%, 12.5%, and 6.25% of PPC of the drug. As published previously^[8], an SI value of ≤ 150 and 150–250 is defined as being highly sensitive and sensitive to the drug, respectively, whereas an SI value of > 250 is defined as being resistant.

Chemotherapy regimens

The chemotherapy drugs and drug combinations used for ATP-TCA testing were as follows: PTX, pegylated liposomal doxorubicin (PLD), topotecan, GEM, PTX + PLD, PLD + oxaliplatin (L-OHP), PTX + nedaplatin (NDP), GEM + NDP, GEM + epirubicin (E-ADM), PTX + ifosfamide (IFO), IFO + E-ADM, etoposide (VP-16) + L-OHP, IFO + VP-16, irinotecan + NDP, and PTX + topotecan + cisplatin. Based on the results of ATP-TCA, the patients in the experimental group were given a chemotherapy regimen with the lowest SI. In the event of two regimens producing similarly strong *in vitro* sensitivity, the physician was requested to select the least toxic alternative. If the best regimen was contraindicated for any reason, the next best regimen was selected at the physician's discretion. For patients in the control group, the chemotherapy regimens were determined by the physician mainly based on the patients' treatment history, side effects, and clinical status, among other factors. The chemotherapeutic dose in both groups was

calculated using a similar method. None of the patients received targeted therapy at this time of recurrence.

Response evaluation

Patients were prospectively monitored for PFS. Serum cancer antigen 125 (CA125) was routinely assessed within 1 week before the start of each cycle of chemotherapy. Computed tomography scanning or magnetic resonance imaging was performed every 2 cycles or when disease progression was suspected based on physical examination or patient symptoms. Patients were regarded as evaluable if a minimum of 2 cycles of chemotherapy were administered. The efficacy was evaluated according to the Response Evaluation Criteria in Solid Tumors^[14] for patients with radiologic relapse and the Rustin criteria^[15] for patients with CA125 elevation only. All chemotherapy regimens were continued for 4–6 cycles in responders and in patients with stable disease. After completion of chemotherapy, all patients were followed up routinely every 3 months through physical examination, serum CA125 evaluation, and imaging examination. The date of the last follow-up was June 24, 2014. PFS was calculated from the start of chemotherapy to progression or lost to follow-up.

Statistical analysis

The SPSS 19.0 software was used to perform statistical analyses. PFS was calculated using the Kaplan-Meier method, and the difference between the experimental group and control groups was analyzed using the log-rank test. Multivariate analysis was conducted using the Cox proportional hazards model. The Fisher exact probability or χ^2 test was used to analyze frequency data. $P < 0.05$ was considered statistically significant.

Results

A total of 86 patients with PRROC were retrospectively analyzed in the present study. Forty-three patients were in the ATP-TCA group, and the other 43 were in the control group. Patients in the control group were selected from the same time period and had the same clinical characteristics as those in the ATP-TCA group. The median age at diagnosis was 53 years. Table 1 shows the clinical and pathological characteristics of all the patients. The specimens utilized in the ATP-TCA test included tumors tissues (30/43, 69.8%) and ascites/pleural effusion aspirate (13/43, 30.2%).

Chemotherapy regimens

The 5 most frequently used regimens in the ATP-TCA group were PTX (paclitaxel) + PLD/E-ADM ($n = 12$), PTX + NDP (nedaplatin) ($n = 10$), PLD + L-OHP ($n = 5$), PTX

Table 1 The clinicopathologic characteristics of all the patients (*n*)

	ATP-TCA	Control
Number of cases	43	43
Median age at diagnosis (years)	55 (26–75)	52 (30–72)
Grade		
2 and 3	42	38
NA	1	5
Histological type		
Serous adenocarcinoma	32	25
Adenocarcinoma	9	16
Clear cell carcinoma	1	1
Transitional cell carcinoma	1	1
Median TFI (months)	3	3
Median No. of prior CT regimens	2 (1–6)	2 (1–6)
Median No. of prior CT cycles	13 (4–32)	15 (4–38)
Secondary cytoreductive surgery		
No surgery/residual disease > 1 cm	22	15
Residual disease ≤ 1 cm	14	14

Note: CT, chemotherapy; NA, not available; PFS, progression free survival; TFI, treatment free interval

+ topotecan + DDP (cisplatin) (*n* = 5), and GEM + NDP/DDP (*n* = 5). Similarly, the 5 most frequently employed chemotherapy regimens in the control group were PTX + NDP (*n* = 10), PTX + PLD (*n* = 5), PLD + L-OHP/NDP (*n* = 5), IFO + E-ADM (*n* = 4), and GEM + NDP/DDP (*n* = 3). Other chemotherapy regimens included the single agent PLD, topotecan, and oral vp16. Table 2 shows the regimens and doses used in the present study. All patients received at least two cycles of chemotherapy after enrollment.

Survival outcomes

After a median follow-up of 13 months (range, 3–46 months), 84 patients experienced relapse or tumor progression, while the other two patients had not yet shown signs of progression until the last follow-up. The overall median PFS was 4 months. The PFS for the ATP-

Table 3 PFS comparison in subgroup analysis

PFS	ATP-TCA (month)	Control (month)	<i>P</i> value
Treatment free interval			
≥ 3 months	7 (<i>n</i> = 25)	4 (<i>n</i> = 25)	0.010
< 3 months	3 (<i>n</i> = 18)	2 (<i>n</i> = 18)	0.353
No. of prior chemotherapy regimen			
1–2	6 (<i>n</i> = 28)	4 (<i>n</i> = 28)	0.025
≥ 3	3 (<i>n</i> = 15)	2 (<i>n</i> = 15)	0.517
Secondary cytoreductive surgery			
No surgery/residual disease > 1 cm	4 (<i>n</i> = 28)	3 (<i>n</i> = 27)	0.025
Residual disease ≤ 1 cm	7 (<i>n</i> = 15)	6 (<i>n</i> = 16)	0.521

TCA group and the control group was 5 and 3 months, respectively (*P* = 0.027). Forty-six patients died of disease, and 40 patients were still alive.

Univariate analysis showed that the prognostic factors for PFS included age (*P* = 0.041), TFI (*P* = 0.012), the number of PCR (*P* = 0.015), treatment (according to ATP-TCA or physician's choice) (*P* = 0.027), and residual disease (patients who did not receive secondary cytoreduction were classified as suboptimal cytoreduction) (*P* = 0.001). The number of cycles of PCR had no impact on PFS (*P* = 0.466). The independent prognostic factors for PFS under multivariate analysis were residual disease [*P* = 0.006; hazard ratio (HR): 2.024, 95% confidence interval (CI): 1.219–3.362] and treatment (*P* = 0.040; HR: 0.623; 95% CI: 0.313–0.973).

Subgroup analysis of PFS

Table 3 summarizes the results of subgroup analysis. The median PFS of patients in the ATP-TCA group and control group who had a TFI of ≥ 3 months (*n* = 50) was 7 and 4 months, respectively (*P* = 0.010) (Fig. 1). Meanwhile, the median PFS for patients in the ATP-TCA group and the control group who had a TFI of < 3 months was 3 and 2 months, respectively (*P* = 0.353).

The median PFS of patients in the ATP-TCA group

Table 2 Mainly used regimens of chemotherapy

Regimen	Dosage
Doxil	40 mg/m ² d1, IV, q4wk
Topotecan	1–1.5 mg/m ² d1, 2, 3, 4, 5, IV, q3wk
Paclitaxel	80 mg/m ² d1, 8,15, IV, q3wk
Epirubicin + paclitaxel	Epirubicin 25 mg/m ² , d1, 2, IV + paclitaxel 175 mg/m ² d1, IV, q3wk
Doxil + paclitaxel	Doxil 25 mg/m ² IV, d1, IV + paclitaxel 175 mg/m ² d1, IV, q3wk
Paclitaxel + nedaplatin	paclitaxel 175 mg/m ² d1, IV + nedaplatin 80 mg/m ² d1, IV, q3wk
Cisplatin + gemcitabine	Cisplatin 75 mg/m ² d1, IV + gemcitabine 1000 mg/m ² d1, 8, IV, q3wk
Nedaplatin + gemcitabine	Nedaplatin 80 mg/m ² d1, IV + gemcitabine 1000 mg/m ² d1, 8, IV, q3wk
Doxil + L-OHP	Doxil 25 mg/m ² IV, d1 + L-OHP 135 mg/m ² d1, IV, q3wk
Doxil + nedaplatin	Doxil 25 mg/m ² IV, d1 + nedaplatin 80 mg/m ² d1, IV, q3wk
Paclitaxel + topotecan + cisplatin	paclitaxel 100 mg/m ² d1, IV + topotecan 1 mg/m ² d1–4, IV + cisplatin 25 mg/m ² , d1, 2, IV, q3wk
Ifosfamide + epirubicin	Ifosfamide 1.5 g/m ² d1–3, IV + epirubicin 25 mg/m ² , d1, 2, IV, q3wk

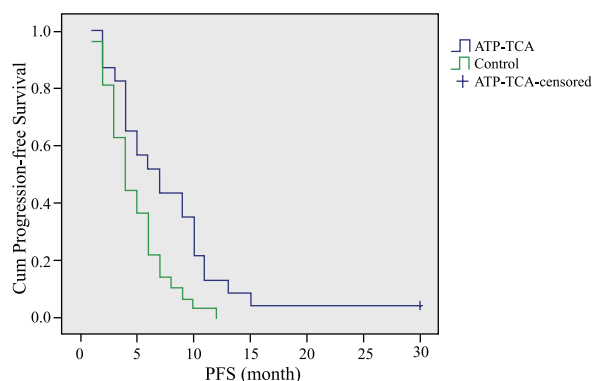


Fig. 1 Comparison of PFS in the subgroup of patients with a TFI of ≥ 3 months ($P = 0.010$)

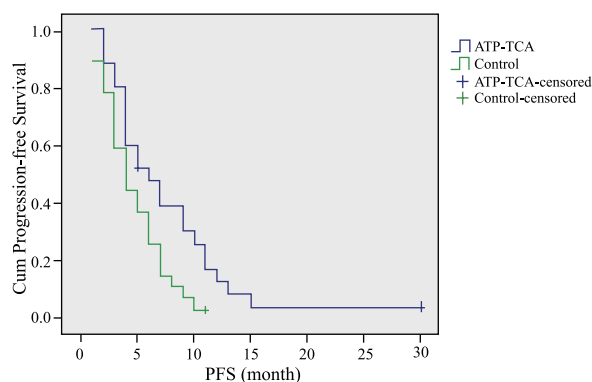


Fig. 2 Comparison of PFS in the subgroup of patients treated with ≤ 2 prior chemotherapy regimens ($P = 0.025$)

and control group who received ≤ 2 cycles of PCR ($n = 52$) was 6 and 4 months, respectively ($P = 0.025$) (Fig. 2). The median PFS for patients in the ATP-TCA group and the control group who received ≥ 3 PCR was 3 and 2 months, respectively ($P = 0.517$).

Among the patients who did not undergo secondary cytoreduction and who experienced suboptimal cytoreduction ($n = 55$), those in ATP-TCA and the control groups had a median PFS of 4 and 3 months, respectively ($P = 0.025$). The patients in the ATP-TCA group and the control group who achieved optimal cytoreduction had a median PFS of 7 and 6 months, respectively ($P = 0.521$).

Discussion

At present, predicting the effective chemotherapeutic regimen for patients based only on the pathological types, grade, history of prior chemotherapy, and other clinical characteristics is difficult. On the other hand, at the molecular level, reliable markers capable of predicting the efficacy of various cytotoxic drugs are still lacking. Thus, any method for testing chemosensitivity is welcome

in the treatment of ROC. Rutherford *et al* reported an improved PFS and OS for patients with ROC treated with chemoresponse assay-sensitive agents [16].

Treatment options for PRROC include multiple cytotoxic agents, such as weekly paclitaxel, GEM, PLD and topotecan, that have different mechanisms of action. ATP-TCA is useful in guiding the selection of optimal chemotherapy regimen. Consistent with a previous study [13], the present study demonstrated that the overall PFS was prolonged in patients with PRROC who received ATP-TCA-directed chemotherapy compared with patients treated based on the physician's choice.

Cree *et al* conducted a prospective, randomized study to determine the response rate and PFS in patients with PRROC who received chemotherapy based on the physician's choice in comparison with ATP-TCA-guided chemotherapy [17]. The results show that the PFS in the ATP-TCA group was slightly but not statistically significantly longer than that in the physician's choice group (104 days vs 93 days, $P < 0.14$). As the number of PCR and cycles increases and the TFI shortens, subsequent chemotherapy would be less effective. For patients with ROC who received ≥ 4 PCR, other cytotoxic drugs are barely active. Any chemosensitivity assay – molecular or cellular – is only as good as the effective drugs that are available. This means that ATP-TCA and other drug-sensitivity testing can theoretically provide no benefit for patients who are resistant to all the cytotoxic agents. Cree *et al* failed to show the statistically significant difference of PFS between the groups possibly because they did not perform a subgroup analysis to exclude the patients with multi-drug resistance.

The subgroup analysis of the present study confirmed that patients who previously received at least 3 chemotherapy regimens (PFS: 3 vs. 2 months, $P = 0.517$) and those with TFI less than 3 months (PFS: 3 vs. 2 months, $P = 0.353$) did not benefit from ATP-TCA. The results of ATP-TCA in the above patient subgroup patients showed that no or few regimens were highly sensitive or sensitive. On the other hand, in patients who had a TFI of ≥ 3 months and previously received only ≤ 2 chemotherapy regimens, ATP-TCA guided chemotherapy prolonged the PFS by 2–3 months compared with the control group. These results provided more indication in selecting patients for ATP-TCA.

The significance of secondary cytoreductive surgery in patients with platinum-resistant cancer was less explored in previous literature. In the present study, among the 37 patients who underwent secondary cytoreduction, 75.7% (28/37) achieved optimal cytoreduction (residual disease < 1 cm). Moreover, multivariate analysis showed that residual disease was an independent prognostic factor in PRROC. Patients with residual disease < 1 cm had better treatment outcome than the others. Among the patients

who achieved optimal cytoreduction, those in the ATP-TCA group had a slightly longer PFS than those in the control group, but the difference was not statistically significant (7 vs. 6 months, respectively). Meanwhile, the PFS of the patients who did not undergo secondary cytoreductive surgery or who failed to achieve optimal cytoreduction was statistically different between the ATP-TCA group and the control group. However, the PFS was only extended by one month (4 vs. 3 months). The role of ATP-TCA in this patient population needs further evaluation.

In the present study, most patients underwent combination chemotherapy because a single agent was less sensitive (higher SI score) than the combination regimens in ATP-TCA. The ratio of patients receiving combination chemotherapy was comparable between the experimental group and the control group. Drug safety between the two groups were not compared in our study because the same doses of chemotherapy were administered in both the experimental and control groups. None of the patients in the present study died due to adverse events.

Conclusions

The ATP-TCA resulted in favorable PFS when used as a predictive assay to individualize chemotherapy regimens in patients with PRROC, particularly in patients who had a TFI of ≥ 3 months and received ≤ 2 PCR. These findings are worth further confirmation via prospective randomized trials.

Acknowledgement

We thank Dr. Ying Huang for her comments on this paper.

Conflict of interest

The authors indicated no potential conflicts of interest.

Informed consent

Informed consent was obtained from all individual participants included in the study.

References

- Gordon AN, Tonda M, Sun S, *et al.* Long-term survival advantage for women treated with pegylated liposomal doxorubicin compared with topotecan in a phase 3 randomized study of recurrent and refractory epithelial ovarian cancer. *Gynecol Oncol*, 2004, 95: 1–8.
- Ferrandina G, Ludovisi M, Lorusso D, *et al.* Phase III trial of gemcitabine compared with pegylated liposomal doxorubicin in progressive or recurrent ovarian cancer. *J Clin Oncol*, 2008, 26: 890–896.
- Rose PG, Blessing JA, Ball HG, *et al.* A phase II study of docetaxel in paclitaxel-resistant ovarian and peritoneal carcinoma: a Gynecologic Oncology Group study. *Gynecol Oncol*, 2003, 88: 130–135.
- Mahner S, Meier W, du Bois A, *et al.* Carboplatin and pegylated liposomal doxorubicin versus carboplatin and paclitaxel in very platinum-sensitive ovarian cancer patients: results from a subset analysis of the CALYPSO phase III trial. *Eur J Cancer*, 2015, 51: 352–358.
- Shoji T, Takatori E, Kaido Y, *et al.* A phase I study of irinotecan and pegylated liposomal doxorubicin in recurrent ovarian cancer (Tohoku Gynecologic Cancer Unit 104 study). *Cancer Chemother Pharmacol*, 2014, 73: 895–901.
- Schrag D, Garewal HS, Burstein HJ, *et al.* American Society of Clinical Oncology Technology Assessment: chemotherapy sensitivity and resistance assays. *J Clin Oncol*, 2004, 22: 3631–3638.
- Morgan RJ Jr, Alvarez RD, Armstrong DK, *et al.* Epithelial ovarian cancer. *J Natl Compr Canc Netw*, 2011, 9: 82–113.
- Sevin BU, Peng ZL, Perras JP, *et al.* Application of an ATP-bioluminescence assay in human tumor chemosensitivity testing. *Gynecol Oncol*, 1988, 31: 191–204.
- Tiersten AD, Moon J, Smith HO, *et al.* Chemotherapy resistance as a predictor of progression-free survival in ovarian cancer patients treated with neoadjuvant chemotherapy and surgical cytoreduction followed by intraperitoneal chemotherapy: a Southwest Oncology Group Study. *Oncology*, 2009, 77: 395–399.
- Joo WD, Lee JY, Kim JH, *et al.* Efficacy of taxane and platinum-based chemotherapy guided by extreme drug resistance assay in patients with epithelial ovarian cancer. *J Gynecol Oncol*, 2009, 20: 96–100.
- Karam AK, Chiang JW, Fung E, *et al.* Extreme drug resistance assay results do not influence survival in women with epithelial ovarian cancer. *Gynecol Oncol*, 2009, 114: 246–252.
- Zhang J, Li H. Heterogeneity of tumor chemosensitivity in ovarian epithelial cancer revealed using the adenosine triphosphate-tumor chemosensitivity assay. *Oncol Lett*, 2015, 9: 2374–2380.
- Gao YT, Wu LY, Zhang W, *et al.* A prospective study of adenosine triphosphate-tumor chemosensitivity assay directed chemotherapy in patients with recurrent ovarian cancer. *Chin J Obstet Gynecol (Chinese)*, 2013, 48: 358–363.
- Therasse P, Arbuck SG, Eisenhauer EA, *et al.* New guidelines to evaluate the response to treatment in solid tumors. European Organization for Research and Treatment of Cancer, National Cancer Institute of the United States, National Cancer Institute of Canada. *J Natl Cancer Inst*, 2000, 92: 205–216.
- Rustin GJ. Use of CA-125 to assess response to new agents in ovarian cancer trials. *J Clin Oncol*, 2003, 21 (10 Suppl): 187S–193S.
- Rutherford T, Orr J Jr, Grendys E Jr, *et al.* A prospective study evaluating the clinical relevance of a chemoresponse assay for treatment of patients with persistent or recurrent ovarian cancer. *Gynecol Oncol*, 2013, 131: 362–367.
- Cree IA, Kurbacher CM, Lamont A, *et al.* A prospective randomized controlled trial of tumor chemosensitivity assay directed chemotherapy versus physician's choice in patients with recurrent platinum-resistant ovarian cancer. *Anticancer Drugs*, 2007, 18: 1093–1101.

DOI 10.1007/s10330-017-0241-1

Cite this article as: Li N, Gao YT, Zhang W, *et al.* Comparative analysis of ATP-based tumor chemosensitivity assay-directed chemotherapy versus physician-decided chemotherapy in platinum-resistant recurrent ovarian cancer. *Oncol Transl Med*, 2017, 3: 225–230.

A retrospective clinical study of neoadjuvant chemotherapy for advanced epithelial ovarian cancer

Yinghui Li, Shaojia Wang, Linlin Yang, Chunmei Yin, Hongying Yang (✉)

Yunnan Cancer Hospital & The Third Affiliated Hospital of Kunming Medical University & Yunnan Cancer Center, Kunming 650000, China

Abstract

Objective The aim of this study was to investigate the clinical efficacy of neoadjuvant chemotherapy (NACT) and the prognostic factors for advanced epithelial ovarian cancer (EOC).

Methods We enrolled 241 patients with stage III and IV EOC who were diagnosed at the Yunnan Cancer Hospital between October 2006 and December 2015. The observation (NACT-IDS) group ($n = 119$) received 1–3 courses of platinum-based NACT, followed by interval debulking surgery (IDS) and 6–8 courses of postoperative chemotherapy. The control group underwent primary debulking surgery (PDS) ($n = 122$) followed by 6–8 courses of postoperative chemotherapy. We analyzed the general conditions of the operations and the survival of both groups.

Results Operating time, intraoperative blood loss and postoperative hospitalization were significantly lower in the NACT-IDS group ($P < 0.05$). The rate of optimal cytoreductive surgery was significantly higher in the NACT-IDS group ($P < 0.05$). A visible residual lesion was observed in 49 (41.18%) and 48 (40%) cases in the NACT-IDS and PDS groups, respectively, which were not significantly different ($P > 0.05$). The percentage of International Federation of Gynecology and Obstetrics (FIGO) stage IV tumors and the recurrence rates were significantly higher in the NACT-IDS group ($P < 0.05$). The mortality rates were 45.19% (47/104) and 35.19% (38/108) in the NACT-IDS and PDS groups, respectively ($P > 0.05$). Progression-free survival was 23.75 ± 9.98 and 23.57 ± 12.25 months in the NACT-IDS and PDS groups, respectively ($P > 0.05$). Overall survival (OS) was 31.11 ± 15.66 and 29.63 ± 18.00 months in the NACT-IDS and PDS groups, respectively ($P > 0.05$). Optimal cytoreductive surgery with or without residual lesion was an independent influencing factor for advanced EOC in multivariate analysis. OS of patients treated with ≥ 8 courses of chemotherapy was significantly longer than those treated with < 8 courses.

Conclusion NACT could improve the intra- and postoperative conditions in advanced EOC patients. Although the percentage of FIGO stage IV cancer was significantly higher in the NACT-IDS group, the prognosis was similar in both the NACT-IDS and PDS groups, suggesting that NACT improves the clinical outcome of advanced EOC. Optimal cytoreductive surgery with no residual lesion is a long-term protective factor in advanced EOC. At least 8 courses of chemotherapy overall or ≥ 6 courses postoperatively improves the OS.

Key words neoadjuvant chemotherapy (NACT); advanced epithelial ovarian cancer (EOC); cytoreduction surgery; prognostic factors

Received: 16 June 2017
Revised: 23 August 2017
Accepted: 27 September 2017

Ovarian cancer is one of the three most common gynecological malignancies and has a high mortality rate. Recently, the incidence of ovarian cancer has increased annually [1]. In 2014, Siegel *et al* [2] reported that 70% of ovarian cancer patients were diagnosed at an advanced stage, with a 5-year overall survival (OS) rate of 44% for all patients and 27% for patients with advanced disease (stage IIIC and IV) with 27%. The treatment of ovarian cancer comprises of primary debulking surgery (PDS),

combined with chemotherapy and other comprehensive treatments. The size of the residual lesion is the main factor affecting prognosis [3–4]. Optimal cytoreductive surgery should, therefore, be performed to improve the quality of life and survival of patients. Patients with advanced epithelial ovarian cancer (EOC) usually have extensive intraperitoneal or distant metastases. Some patients have large pelvic masses that adhere tightly to other organs and tissues, and only 30–40% of these patients can be treated

with optimal cytoreductive surgery [5]. Neoadjuvant chemotherapy (NACT) is proposed in advanced EOC to reduce tumor burden, which may ensure the feasibility of optimal cytoreductive surgery in these patients. This strategy has attracted a lot of attention from clinicians. However, whether NACT improves the quality of life and prolongs progression-free survival (PFS) and OS in advanced EOC is still controversial.

We analyzed the clinical importance of NACT in 241 patients with advanced EOC who were diagnosed and treated at the Yunnan Cancer Hospital from October 2006 to December 2015. We have also determined the possible prognostic factors and hope that our study can be used as a reference for the diagnosis and treatment of EOC patients.

Materials and methods

Patients

We enrolled 241 patients who were diagnosed with advanced EOC (178 stage III and 63 stage IV) between October 2006 and December 2015 at the Yunnan Cancer Hospital. Patients were divided into two groups according to treatment modality: 119 underwent NACT-interval debulking surgery (IDS), and 122 underwent PDS. The observation (NACT-IDS) group ($n = 119$) received 1–3 courses of platinum-based NACT, followed by IDS and 6–8 courses of postoperative chemotherapy. The control (PDS) group underwent PDS ($n = 122$) followed by 6–8 courses of postoperative chemotherapy. All patients received platinum-based chemotherapy: TC (paclitaxel: 175 mg/m², intravenous injection; carboplatin: AUC 5–6, intravenous injection, once every 3 weeks); or TP (paclitaxel: 175 mg/m² intravenous injection; cisplatin: 75 mg/m² intravenous injection, once every 3 weeks). We analyzed age, body mass index (BMI), clinical manifestations, surgical pathological stage, histopathological type, days of hospitalization, days in intensive care, operating time, intraoperative blood loss and transfusion, presence of residual lesions, percentage of patients undergoing cytoreductive surgery, postoperative complications, and effect of NACT on operation, PFS, and OS.

Data analysis

Statistical analysis was performed using the Stata version 12.0 software. Data were analyzed using t test or χ^2 test, and $P < 0.05$ was defined as statistically significant. Survival analysis was performed using the log-rank test and Kaplan-Meier test. Multivariate analysis was performed using the Cox model.

Results

General situation

The general conditions of patients including age, BMI, clinical manifestations, histopathological type and pathological differentiation, were comparable among patients in the NACT-IDS and PDS groups ($P > 0.05$; Table 1). However, surgical pathological stages differed significantly between the two groups ($P < 0.05$).

Surgical condition

The average operating time, intraoperative blood loss, and days of hospitalization were significantly lower in the NACT-IDS group compared to the PDS group ($P < 0.05$; Table 2). There were no significant differences in the intraoperative blood transfusion rates, postoperative days in intensive care and postoperative complications between the groups ($P > 0.05$). A higher percentage of patients in the NACT-IDS group underwent optimal cytoreductive surgery compared to the PDS group (69.75% vs 59.30%, $P < 0.05$). The percentage of patients with a visible residual lesion was comparable in both groups (NACT-IDS: 41.18%; PDS: 40.0%).

Survival analysis

The duration of follow-up ranged from 15 to 125 months. The recurrence rate was 58.04% (65/112) in the NACT-IDS group and 36.28% (41/113) in the PDS group ($P < 0.05$). The morbidity was 45.19% (47/104) in the NACT-IDS group and 35.19% (38/108) in the PDS group ($P < 0.05$). The median PFS and OS for the NACT-IDS group were 23.75 ± 9.98 and 31.11 ± 15.66 months, respectively, compared with 23.57 ± 12.25 and 29.63 ± 18.0 months, respectively, for the PDS group. However, these differences were not significant ($P > 0.05$; Fig. 1 and 2, Table 3).

Prognostic factors

Univariate analysis showed that age, BMI, comorbidity, pathological grade, residual lesion size, and ascites were not significantly associated with PFS ($P > 0.05$). On the other hand, histopathological type, visible residual lesion, total number of cycles of chemotherapy, and number of cycles of postoperative chemotherapy were significantly associated with PFS ($P < 0.05$). Patients with no visible residual lesion, ≥ 8 cycles of chemotherapy or ≥ 6 cycles of postoperative chemotherapy had improved PFS. Histopathological type demonstrated a hazard ratio (HR) of 3.999 [95% confidence interval (CI) 1.7813–8.9818] for mucinous carcinoma, 1.1020 (95% CI 0.6820–1.7806)

Table 1 Comparison of the two groups in general

Characteristic	NACT-IDS group (n = 119)	PDS group (n = 122)	t/ χ^2	P
Age (years)	52.36 ± 8.58	52.00 ± 8.69	-0.3174	0.7512
BMI	22.27 ± 3.46	22.13 ± 2.77	2.9297	0.270
Clinical manifestations			8.4555	0.076
Abdominal distension and abdominal pain	97	94		
Physical examination	6	10		
Irregular vaginal bleeding	1	8		
Consciously abdominal mass	11	9		
Other (chest tightness, fatigue, weight loss, frequent urination, urgency, etc.)	4	1		
Surgical pathology			21.7144	0.000
III	72 (0.50%)	106 (86.88%)		
IV	47 (39.49%)	16 (13.11%)		
Histopathological type			21.8478	0.000
Serous carcinoma	64	81		
Mucinous carcinoma	0	10		
Endometriosis	54	34		
Transparent cell carcinoma	0	5		
Hybrid	0	2		
Histopathological grade			0.3187	0.853
Well differentiated	2	3		
Differentiation	15	16		
Poorly differentiated	76	72		
Unknown	26	31		

Table 2 Comparison of the two groups of patients

Characteristic	NACT-IDS group	PDS group	t/ χ^2	P
Number of days of hospitalization (days)	19.59 ± 5.46	22.16 ± 7.11	3.1373	0.0019
Intensive care time (days)	0.09 ± 0.52	0.26 ± 0.95	1.7128	0.088
Surgery time (min)	201.75 ± 61.41	235.26 ± 81.72	3.5458	0.0005
Intraoperative blood loss (mL)	496.66 ± 414.50	637.43 ± 648.03	1.9889	0.0479
Intraoperative blood transfusion			-1.6588	0.0985
Yes	25 (21.19%)	37 (30.58%)		
No	93 (78.81%)	84 (69.42%)		
Visible lesion			0.0343	0.853
No visible remnants of the naked eye	49 (41.18%)	48 (40%)		
See the remnants of the naked eye	70 (58.82%)	72 (60%)		
Ideal tumor cell subtraction (example)			4.6158	0.032
Ideal tumor cell subtraction	83 (69.75%)	67 (56.30%)		
Not ideal for tumor cell ablation	36 (30.25%)	52 (43.70%)		
Postoperative complications (example)			2.1566	0.142
No	107 (51.46%)	101 (83.47%)		
Yes	12 (37.5%)	20 (16.53%)		

Table 3 Comparison of survival results between the two groups

Characteristic	NACT-IDS group	PDS group	t/χ^2	<i>P</i>
Relapse			10.6818	0.001
Yes	65 (58.04%)	41 (36.28%)		
No	47 (41.06%)	72 (63.72%)		
Death			2.2090	0.137
Yes	47 (45.19%)	38 (35.19%)		
No	57 (54.81%)	70 (64.81%)		
PFS (months)	23.75 ± 9.98	23.57 ± 12.25	-0.1232	0.902
OS (months)	31.11 ± 15.66	29.63 ± 18.00	-0.6335	0.5271
Median survival (months)	45	50	0.7400	0.3904

Table 4 Single factor analysis of PFS

Factor	<i>n</i>	OR	95% CI	t/χ^2	<i>P</i>
Age (years)				2.16	0.5392
BMI				0.65	0.4198
Complications				3.93	0.2687
Pathology type				24.93	0.0001
Serous carcinoma	135				
Mucinous carcinoma	10	3.9999	1.7813–8.9818		
Endometriosis	88	1.1020	0.6820–1.7806		
Transparent cell carcinoma	5	16.1711	6.0525–43.2060		
Hybrid	2	2.0395	0.2792–14.8944		
Pathology differentiation				2.87	0.0902
Visually visible lesions				5.00	0.0253
Yes	142				
No	97	0.5977	0.3765–0.9488		
Residual lesion size				3.75	0.0529
< 1	150	0.6432	0.4139–0.9995		
≥ 1	88				
Postoperative chemotherapy (Total chemotherapy cycle number ≥ 8 months)				16.70	0.0000
Carry out	104	0.3864	0.2394–0.6236		
Undone	129				
Postoperative chemotherapy cycles				4.10	0.0302
≥ 6	150	0.6173	0.4007–0.9510		
< 6	91				
Ascites cytology				0.41	0.5191
Positive	106				
Negative	93				

for endometrial carcinoma, and 16.1711 (95% CI 6.0525–43.2060) for clear cell carcinoma when compared with serous carcinoma, which suggested worse prognosis (Table 4; $P < 0.05$).

Patients with no visible residual lesion or postoperative residual lesions < 1 cm, ≥ 8 cycles of chemotherapy and ≥ 6 cycles of postoperative chemotherapy had improved OS

($P < 0.05$). Histopathological type showed an HR of 3.2483 (95% CI 1.4287–7.3854) for mucinous carcinoma, 1.1540 (95% CI 0.7113–1.8721) for endometrial carcinoma, and 18.1405 (95% CI 6.5994–49.8648) for clear cell carcinoma when compared with serous carcinoma, which suggested worse prognosis (Table 5, Fig. 3–6).

Significant factors from the univariate analyses were

Table 5 Univariate analysis of OS

Fator	<i>n</i>	OR	95% CI	<i>t/χ²</i>	<i>P</i>
Age (years)				0.74	0.3885
BMI				1.21	0.2722
Complications				2.75	0.0973
Pathology type				24.05	0.0001
Complications	135				
Pathology type	10	3.2483	1.4287–7.3821		
Complications	88	1.1540	0.7113–1.8721		
Pathology type	5	18.1405	6.5994–49.8648		
Complications	2	3.3455	0.4533–24.6892		
Visually visible lesions				8.09	0.0044
Yes	142				
No	97	0.5057	0.3109–0.8225		
Residual lesion size				5.48	0.0192
< 1	150	0.5805	0.3707–0.9090		
≥ 1	88				
Postoperative chemotherapy (Total chemotherapy cycle number ≥ 18 months)				22.58	0.0000
Carry out	104	0.3864	0.2394–0.6236		
Undone	129				
Postoperative chemotherapy cycles				9.90	0.0017
≥ 6	150	0.6173	0.4007–0.9510		
< 6	91				
Ascites cytology				1.43	0.2312
Positive	106				
Negative	93				

Table 6 Multi-factor analysis of OS

Fator	OR	Stand error	95% CI	<i>P</i>
Age	0.9638	0.1700	0.6821–1.3618	0.834
BMI	1.4413	0.3197	0.9332–2.2262	0.099
Pathology type	1.0154	0.1567	0.7505–1.3740	0.921
Pathology grade	0.7660	0.3196	0.3381–1.7354	0.523
Visually visible lesions	0.3457	0.1564	0.1424–0.8391	0.019
Residual lesion size	0.5572	0.2132	0.2633–1.1795	0.126
Complete postoperative chemotherapy (Total chemotherapy cycle number ≥ 8 months)	0.2551	0.1004	0.1180–0.5519	0.001
Postoperative chemotherapy cycles	0.8929	0.3322	0.4307–1.8514	0.761
Surgical pathology	0.7819	0.2957	0.3726–1.6406	0.515

selected for multivariate analysis. Presence of visible residual lesion and the number of postoperative cycles of chemotherapy were independent factors for OS in patients with advanced EOC (*P* < 0.05; Table 6). The

number of cycles of postoperative chemotherapy was the only independent factor for PFS in patients with advanced EOC (*P* < 0.05; Table 7).

Table 7 Multivariate analysis of OS

Fator	OR	Stand error	95% CI	P
Age	0.9849	0.1722	0.6991–1.3875	0.931
BMI	1.3227	0.2845	0.8677–2.0164	0.194
Pathology type	0.9361	0.1411	0.6966–1.2580	0.661
Pathology grade	0.5812	0.2386	0.2600–1.2994	0.186
Visually visible lesions	0.6837	0.2765	0.3094–1.5105	0.347
Residual lesion size	0.6301	0.2371	0.3014–1.3174	0.220
Complete postoperative chemotherapy (Total chemotherapy cycle number \geq 8 months)	0.3478	0.1257	0.1712–0.7064	0.003
Postoperative chemotherapy cycles	1.0877	0.3774	0.5510–2.1473	0.809
Surgical pathology	0.8214	0.2932	0.4080–1.6536	0.582

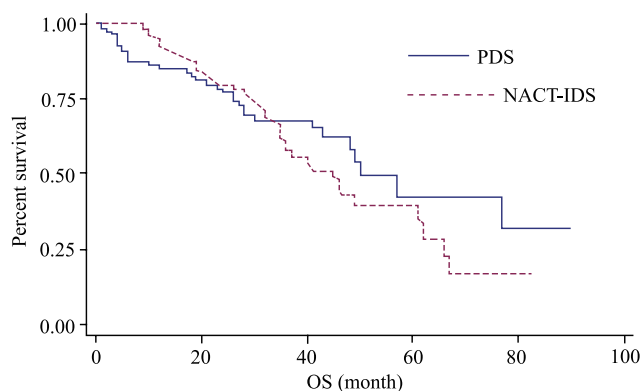


Fig. 1 OS of the two groups.

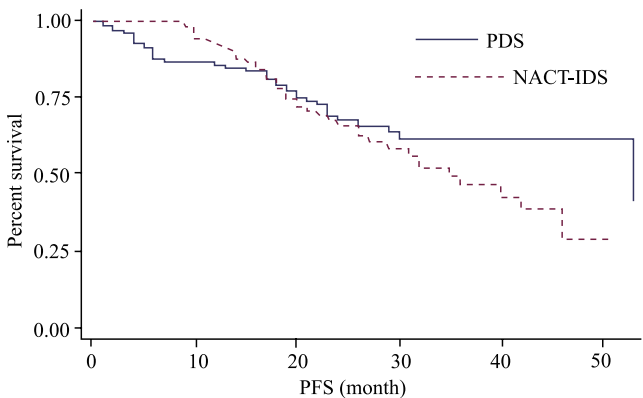


Fig. 2 PFS of the two groups.

Discussion

Ovarian cancer is one of the three most common gynecological malignancies and its incidence has been increasing in the recent years. Epithelial carcinoma is the most common pathological type of ovarian cancer [6], and about 70% of patients are diagnosed with stage

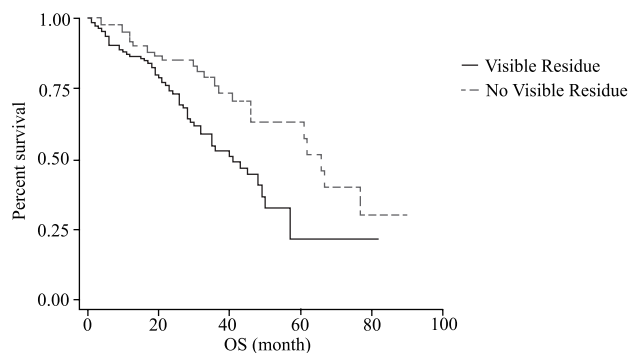


Fig. 3 visible residual lesion.

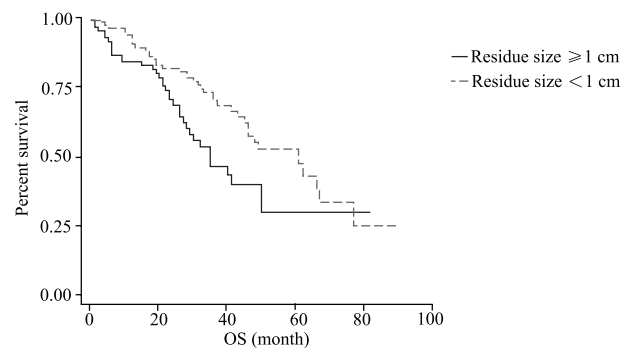


Fig. 4 residual lesion size.

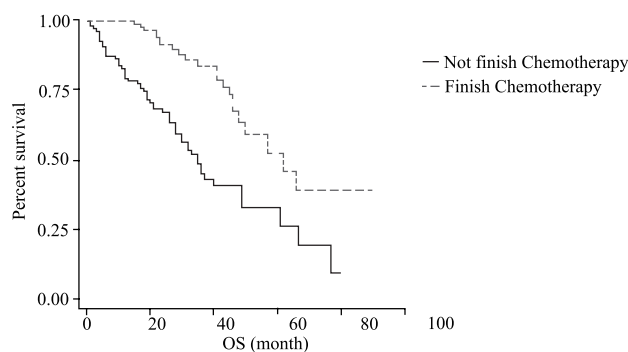


Fig. 5 postoperative chemotherapy.

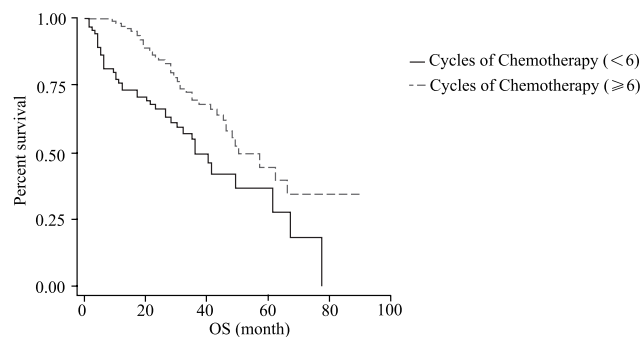


Fig. 6 postoperative chemotherapy cycles.

III or IV cancer. At present, the principal treatment for ovarian cancer is still cytoreductive surgery, combined with chemotherapy and other comprehensive treatments [7]. Although treatment strategies for EOC have improved, only 45% of the patients can undergo optimal cytoreductive surgery [8]. NACT is recognized by an increasing number of clinicians, but the 5-year survival rate for advanced ovarian cancer patients following NACT is only 30%–55% [9]. A clinical study has shown that compared to PDS, NACT-IDS ensures more patients can be treated using optimal cytoreductive surgery, with an improved quality of life. Whether NACT-IDS can improve prognosis needs further investigation [10].

National Comprehensive Cancer Network (NCCN) guidelines recommend the removal of all visible lesions, and an EORTC–NCIC study showed that an absence of visible lesions is the most important factor for better prognosis of advanced EOC [11]. NACT is an alternative option for patients with advanced EOC, especially those who cannot be treated with optimal cytoreductive surgery [12]. The results of this study show that the ideal tumor reduction rate in the NACT-IDS group was 69.75%, which was higher than that in the PDS group (56.30%), and NACT significantly improved the surgical outcomes in advanced ovarian epithelial carcinoma. In our study, 41.18% and 40.0% of patients in the NACT-IDS and PDS groups, respectively had no visible residual lesions, which was not a significant difference. It has been shown that NACT effectively reduces the tumor burden and induces tumor shrinkage [13–16], which leads to better conditions for optimal cytoreduction surgery [17]. In recent years, an increasing number of researchers have defined optimal cytoreductive surgery as the absence of visible residual lesions. A study by Cochrane confirmed that the HR was lower in patients with no visible residual lesions, thereby suggesting that removal of all visible lesions may prolong patient survival [18–22]. Moreover, in our study, NACT shortened hospitalization and operating times and reduced the intraoperative blood loss. Several studies have confirmed the feasibility and efficacy of NACT-IDS

regimens in advanced EOC patients, which have been recognized by most experts [23].

As NACT can improve surgery, we speculated whether it could also improve the prognosis of advanced EOC. EORTC55971 [24] is an international, multicenter, randomized controlled phase III clinical trial involving 59 countries with a total of 670 patients. The results showed that postoperative complications (such as infection, bleeding, and venous thromboembolism) in the NACT-IDS group were significantly fewer than in the PDS group, yet there was no significant difference in OS and PFS. Even when the size of the residual lesion and patient's age were considered, the results remained unchanged. In the follow-up study by Fago-Olsen [25], there was no difference in the median survival time between these two groups. The median survival time of patients with no visible lesions in the PDS group was longer, and the 2-year mortality HR increased in the NACT-IDS group when compared with the PDS group.

Kehoe *et al* performed a non-inferiority, multicenter, phase III randomized controlled trial of NACT in patients with advanced EOC. Although NACT increased the chances of a successful optimal cytoreductive surgery and reduced surgical complications and mortality, it did not improve prognosis. Although several clinical trials have demonstrated that NACT has no significant beneficial effect on OS and PFS when compared with PDS [26–31], some studies have reported a different effect. A study conducted in Yale University School of Medicine showed that patients with extraperitoneal metastases who received NACT had an OS and PFS of 31 and 15 months, respectively, which were significantly higher than those in patients treated with traditional strategies [32].

A meta-analysis of 21 retrospective clinical studies showed that NACT did not prolong the median survival time when compared with PDS, although the optimal cytoreductive surgery rate increased [33]. The results seemed to be contradictory to some extent because there may have been some bias in the retrospective studies. Patients treated with NACT had severe late International Federation of Gynecology and Obstetrics (FIGO) stage cancer, large tumor volume and extensive disease. Consistent with previous studies, we also found that PFS did not differ significantly between the NACT-IDS and PDS groups. However, the percentage of patients with FIGO stage IV cancer in the NACT-IDS group was significantly higher than that in the PDS group (39.49% vs. 13.11%), which could account for the similar PFS and OS. This finding suggests that the NACT-IDS regimen may improve the prognosis of advanced EOC.

In our study, the recurrence rates were 58.04% and 36.28% in the NACT-IDS and PDS groups, respectively. Four factors may have contributed to these results: (1) retrospective clinical studies can be selectively biased;

(2) postoperative residual lesion size measurement can be biased; (3) chemotherapy-resistant patients benefit little from NACT and may have a poor prognosis because they are unable to undergo optimal cytoreductive surgery; (4) presence of cell fibrosis after NACT. It has been reported that tumor stem cells, leading to tumor recurrence, may still be present in fibrotic tissue after NACT [34–35]. More studies are urgently needed to explore the underlying mechanisms.

The effect of age on the prognosis of advanced EOC differs among studies. While some studies demonstrated no association between age and prognosis [36–37], a Danish study of ovarian cancer suggested that age is an important factor for OS [38]. In our study, the onset age of patients was not significantly associated with PFS and OS. Compared with the 51–61-years group (high incidence group in our study), the prognosis in patients aged 29–39 and 62–73 years was poor. As an increasing number of younger women have EOC, comprehensive treatment strategies with individualized considerations will be beneficial.

Most researchers believe that EOC with different pathological characteristics may lead to different prognosis. Bamias *et al* [39] found that serous carcinoma (367 cases, 47.7 months), mucinous carcinoma (24 cases, 15.4 months), and clear cell carcinoma (29 cases, 36.6 months) were significantly different. Two other similar studies found that a serous type pathology was a detrimental prognostic factor [40–41]. The results of our study show that mucinous carcinoma and clear cell carcinoma predict worse prognosis in univariate analysis. Although there was no significant difference in OS, mucinous carcinoma and clear cell carcinoma showed a higher malignant potential. A large number of studies have shown that the prognosis of early mucinous carcinoma is better than that of the serous type. However, our results differed because of the biological characteristics of the advanced mucinous carcinoma—extensive lesions were found in the bowel and peritoneum—which suggest difficulty in surgical removal of the entire tumor, and a high risk of distant metastasis.

In our study, the histopathological grade was not a prognostic factor for PFS and OS. It is believed that a poorly differentiated tumor has a stronger invasive ability that may lead to a poorer prognosis. We did not confirm this in our study, but this may have been because of the sample size. NCCN guidelines advocate optimal cytoreductive surgery to remove all visible lesions or reduce the residual lesions to <1 cm. It has been shown that the postoperative residual lesion size is an independent prognostic factor that adversely affects the prognosis of EOC patients [42–43] and our findings conform with these reports. Several studies have shown that patients who undergo suboptimal cytoreductive surgery have a shorter survival time. On the other hand, even patients diagnosed with FIGO stage IV cancer can benefit

from optimal cytoreductive surgery [44–46].

The principal treatment for EOC is optimal cytoreductive surgery with adequate, standardized chemotherapy. The current NCCN guidelines recommend six courses of chemotherapy after surgery. Our findings are consistent with several other studies that have shown that delayed or interrupted postoperative chemotherapy and < 6 cycles of chemotherapy lead to recurrence and poor prognosis [47–49]. Timeous and adequate postoperative chemotherapy were favorable prognostic factors for PFS and OS in advanced EOC patients in both univariate and multivariate analysis. Patients treated with ≥ 6 cycles of chemotherapy each before and after surgery had a better prognosis.

In conclusion, in patients with EOC, NACT can help in preparing them for cytoreductive surgery, as well as improve their surgical outcomes. Even though the number of patients with FIGO stage IV cancer was significantly higher in the NACT-IDS group compared to that in the PDS group, the two groups showed comparable PFS, OS, and mortality, suggesting that NACT can improve the prognosis of advanced EOC. Optimal cytoreductive surgery with no visible residual lesions should be advocated in clinical practice. Treatment with ≥ 6 cycles of postoperative chemotherapy or with ≥ 8 cycles of chemotherapy in total results in a better prognosis. Advanced EOC patients should be evaluated based on their general situation, histopathological types of tumor, and considered for surgery by a gynecological oncologist before treatment. Appropriate, adequate, individualized chemotherapy regimens could improve the quality of life and survival of these patients.

Acknowledgement

We thank Cathel Kerr, PhD, from Liwen Bianji, Edanz Editing China (www.liwenbianji.cn/ac), for editing the English text of a draft of this manuscript.

Conflicts of interest

The authors indicated no potential conflicts of interest.

References

1. Fotopoulou C, Savvatis K, Steinhagen-Thiessen E, *et al*. Primary radical radical surgery in elderly patients with epithelial ovarian cancer: analysis of surgical outcome and long-term survival. *Int J Gynecol Cancer*, 2010, 20: 3–40.
2. Siegel R, Ma J, Zou Z, *et al*. Cancer statistics, 2014. *CA Cancer J Clin*, 2014, 64: 9–29.
3. Elattar A, Bryant A, Winter-Roach BA, *et al*. Optimal primary surgical treatment for advanced epithelial ovarian cancer. *Cochrane Database Syst Rev*, 2011: 7565.
4. du Bois A, Reuss A, Harter P, *et al*. Potential role of lymphadenectomy

- in advanced ovarian cancer: a combined exploratory analysis of three prospectively randomized phase III multicenter trials. *J Clin Oncol*, 2010, 28: 1733–1739.
5. Vergote I, du Bois A, Amant F, *et al*. Neoadjuvant chemotherapy in advanced ovarian cancer: On what do we agree and disagree. *Gynecol Oncol*, 2013, 128: 6–11.
 6. Hu ZH, Zheng R, Du C. Clinical observation of TP regimen neoadjuvant chemotherapy in the treatment of 38 patients with advanced ovarian cancer. *Chinese Med Guide (Chinese)*, 2013, 11: 47–49.
 7. Chereau E, Lavoue V, Ballester M, *et al*. External validation of a laparoscopic-based score to evaluate resectability for patients with advanced ovarian cancer undergoing interval debulking surgery. *Anticancer Res*, 2011, 31: 4469–4474.
 8. López-Guerrero JA, Romero I, Poveda A. Trabectedin therapy as an emerging treatment strategy for recurrent platinum-sensitive ovarian cancer. *Chin J Cancer*, 2015, 34: 41–49.
 9. Poveda A, Ray-Coquard I, Romero I, *et al*. Emerging treatment strategies in recurrent platinum-sensitive ovarian cancer: focus on trabectedin. *Cancer Treat Rev*, 2014, 40: 366–375.
 10. Diener KR, Al-Dasooqi N, Lousberg EL, *et al*. The multifunctional alarmin HMGB1 with roles in the pathophysiology of sepsis and cancer. *Immunol Cell Biol*, 2013, 91: 443–450.
 11. Vergote I, Trope CG, Amant F, *et al*. Neoadjuvant chemotherapy or primary surgery in stage IIIC-IV ovarian cancer. *New England J Med*, 2010, 363: 943–953.
 12. Morrison J, Haldar K, Kehoe S, *et al*. Chemotherapy versus surgery for initial treatment in advanced ovarian epithelial cancer. *Cochrane Database Syst Rev*, 2014: CD005343. doi: 10.1002/14651858.CD005343. pub3.
 13. Vergote I, du Bois A, Arant F, *et al*. Neoadjuvant chemotherapy in advanced ovarian cancer: On what do we agree and disagree? *Gynecol Oncol*, 2013, 128: 6–11.
 14. Vergote I, De Wever I, Tjalma W, *et al*. Neoadjuvant chemotherapy or primary debulking surgery in advanced ovarian carcinoma: a retrospective analysis of 285 patients. *Gynecol Oncol*, 1998, 71: 431–436.
 15. Hou JY, Kelly MG, Yu H, *et al*. Neoadjuvant chemoth lessens surgical morbidity in advanced ovarian cancer and leads to improved in stage IV disease. *Gynecol Oncol*, 2007, 105: 211–217.
 16. Everett EN, French AE, Stone RL, *et al*. Initial chemotherapy followed by surgical cytoreduction for the treatment of stage III/IV epithelial ovarian cancer. *Am J Obstet Gynecol*, 2006, 195: 568–574.
 17. Shang L. Clinical study of neoadjuvant chemotherapy and surgery for advanced ovarian cancer. *Ningxia Med J (Chinese)*, 2011, 33: 618–619.
 18. Bristow RE, Tomacruz RS, Armstrong DK, *et al*. Survival effect of maximal cytoreductive surgery for advanced ovarian carcinoma during the platinum era: a meta-analysis. *J Clin Oncol*, 2002, 20: 1248–1259.
 19. du Bois A, Reuss A, Pujade-Lauraine E, *et al*. Role of surgical outcome as prognostic factor in advanced epithelial ovarian cancer: a combined exploratory analysis of 3 prospectively randomized phase 3 multicenter trials: by the Arbeitsgemeinschaft Gynaekologische Onkologie Studiengruppe Ovarialkarzinom (AGO-OVAR) and the Groupe d'Investigateurs Nationaux Pour les Etudes des Cancers de l'Ovaire (GINECO). *Cancer*, 2009, 115: 1234–1244.
 20. Polterauer S, Vergote I, Concin N, *et al*. Prognostic value of residual tumor size in patients with epithelial ovarian cancer FIGO stages IIA-IV: analysis of the OVCAD data. *Int J Gynecol Cancer*, 2012, 22: 384–385.
 21. Winter WE 3rd, Maxwell GL, Tian C, *et al*. Prognostic factors for stage III epithelial ovarian cancer: a Gynecologic Oncology Group Study. *J Clin Oncol*, 2007, 25: 3621–3627.
 22. Winter WE 3rd, Maxwell GL, Tian C, *et al*. Tumor residual after surgical cytoreduction in prediction of clinical outcome in stage IV epithelial ovarian cancer: a Gynecologic Oncology Group Study. *J Clin Oncol*, 2008, 26: 83–89.
 23. Diener KR, Al-Dasooqi N, Lousberg EL, *et al*. The multifunctional alarmin HMGB1 with roles in the pathophysiology of sepsis and cancer. *Immunol Cell Biol*, 2013, 91: 443–450.
 24. Morrison J, Swanton A, Collins S, *et al*. Chemotherapy versus surgery for initial treatment in advanced ovarian epithelial cancer. *Cochrane Database Syst Rev*, 2012: CD005343. doi: 10.1002/14651858.CD005343. pub2.
 25. Fagö-Olsen CL, Ottesen B, Kehkt H, *et al*. Do neoadjuvant chemotherapy impair long-term survival for ovarian cancer patients. A nationwide Danish study. *Gynecol Oncol*, 2014, 132: 292–298.
 26. Hou JY, Kelly MG, Yu H, *et al*. Neoadjuvant chemotherapy lessens surgical morbidity in advanced ovarian cancer and leads to in stage IV disease. *Gynecol Oncol*, 2007, 105: 211–217.
 27. Everett EN, French AE, Stone RL, *et al*. Initial chemotherapy followed by surgical cytoreduction for the treatment of stage IV epithelial ovarian cancer. *Am J Obstet Gynecol*, 2006, 195: 568–574.
 28. Joseph NT, Pepin KJ, Alejandro Rauh-Hain J, *et al*. Mass General Ovarian Cancer: A Comparison with the CHORUS Trial. *Gynecol Oncol*, 2015, 139: 589–590.
 29. Loizzi V, Cormio G, Resta L, *et al*. Neoadjuvant chemotherapy in advanced ovarian cancer: a case-control study. *Int J Gynecol Cancer*, 2005, 15: 217–223.
 30. Steed H, Oza AM, Murphy J, *et al*. A retrospective analysis of neoadjuvant platinum-based chemotherapy versus up-front surgery in advanced ovarian cancer. *Int J Gynecol Cancer*, 2006, 16 (Supp11): 47–53.
 31. Xu ZM, Zong LL, Zhao L, *et al*. Clinical Observation of neoadjuvant chemotherapy combined with cytoreductive surgery in the treatment of advanced epithelial ovarian cancer. *Shandong Med (Chinese)*, 2015, 139: 589–590.
 32. Hou JY, Kelly MG, Yu H, *et al*. Neoadjuvant chemotherapy lessens surgical morbidity in advanced ovarian cancer and leads to improved survival in stage IV disease. *Gynecol Oncol*, 2007, 105: 211–217.
 33. Suidan RS, Ramirez PT, Sarasohn DM, *et al*. A multicenter prospective trial evaluating the ability of preoperative computed tomography scan and serum CA-125 to predict suboptimal cytoreduction at primary debulking surgery for advanced ovarian, fallopian tube, and peritoneal cancer. *Gynecol Oncol*, 2014, 134: 455–461.
 34. Kang S, Nam BH. Does neoadjuvant chemotherapy increase optimal cytoreduction rate in advanced ovarian cancer. *Meta-analysis of 21 studies. Ann Surg Oncol*, 2009, 16: 2315–2320.
 35. Lim MC, Song YJ, Seo SS, *et al*. Residual cancer stem cells after interval cytoreductive surgery following neoadjuvant chemotherapy could result in poor treatment outcomes for ovarian cancer. *Onkologie*, 2010, 33: 324–330.
 36. Tang L, Zheng M, Xiong Y, *et al*. Clinical characteristics and prognosis of epithelial ovarian cancer in young women. *Cancer*, 2008, 27: 951–955.
 37. Liu K, Chen HX, Zhang H. Prognostic factors of advanced ovarian cancer. *Prog Mod Obstet Gynecol (Chinese)*, 2012, 19: 9–12.
 38. Carsten C, Ottesen B, Kehlet H, *et al*. Does neoadjuvant chemotherapy impair long-term survival for ovarian patients? A nationwide Danish study. *Gynecol Oncol*, 2014, 132: 292–298.

39. Bamias A, Psaltopoulou T, Sotiropoulou M, *et al.* Mucinous but not clear cell histology is associated with inferior survival in patients with advanced stage ovarian carcinoma treated with platinum-paclitaxel chemotherapy. *Cancer*, 2010,116: 1462–1468.
40. Alexandre J, Ray-Coquard I, Selle F, *et al.* Mucinous advanced epithelial ovarian carcinoma: clinical presentati and sensitivity to platinum-paclitaxel-based chemotherapy, the GINECO experience. *Ann Oncol*, 2010, 21: 2377–2381.
41. Zaino RJ, Brady MF, Lele SM, *et al.* Advanced stage mucinous adenocarcinoma of the ovary is both rare and highly lethal: a Gynecologic Oncology Group study. *Cancer*, 2011, 117: 554–562.
42. Arikan SK, Kasap B, Yetimalar H, *et al.* Impact of prognostic factors on survival rates in patients with ovarian carcinoma. *Asian Pac J Cancer Prev*, 2014, 15: 6087–6094.
43. Akesson M, Jakobsen AM, Zetterqvist BM, *et al.* A population-based 5-year cohort study including all cases of epithelial ovarian cancer in western Sweden: 10-year survival and prognostic factors. *Int J Gynecol Cancer*, 2009, 19:116–123.
44. Skirisdottir I, Sorbe B. Prognostic factors for surgical outcome and survival in 447 women treated for advanced (FIGO-stages III-IV) epithelial ovarian carcinoma. *Int J Oncol*, 2007, 30: 727–734.
45. Terauchi F, Nishi H, Moritake T, *et al.* Prognostic factor on optimal debulking surgery by maximum effort for stage IIIC epithelial ovarian cancer. *J Obstet Gynaecol Res*, 2009, 35: 315–319.
46. Wimberger P, Wehling M, Lehmann N, *et al.* Influence of residual tumor on outcome in ovarian cancer patients with FIGO stage IV disease: an exploratory analysis of the AGO-OVAR (Arbeitsgemeinschaft Gynaekologische Onkologie Ovarian Cancer Study Group). *Ann Surg Oncol*, 2010,17: 1642–1648.
47. Harries M, Gore M. Part 1: chemotherapy for epithelial ovarian cancer-treatment at first diagnosis. *Lancet Oncol*, 2002, 3: 529–536.
48. Kim HS, Park NH, Chung HH, *et al.* Are three additional cycles of chemotherapy useful in patients with advanced-stage epithelial ovarian cancer after a complete response to six cycles of intravenous adjuvant paclitaxel and carboplatin? *Jpn J Clin Oncol*, 2008, 38: 445–450.
49. González-Martin A, GEICO Group. Treatment of recurrent disease:randomized trials of monotherapy versus combination chemotherapy. *Int J Gynecol Cancer*, 2005,15 (Suppl 3): 241–246.

DOI 10.1007/s10330-017-0242-2

Cite this article as: Li YH, Wang SJ, Yang LL, *et al.* A retrospective clinical study of neoadjuvant chemotherapy for advanced epithelial ovarian cancer. *Oncol Transl Med*, 2017, 3: 231–240.

Effect of parathyroid hormone on apoptosis of human medullary thyroid carcinoma cells*

Xiaofeng Hou, Qinjiang Liu (✉), Youxin Tian

Department of Head and Neck Surgery, The Cancer Hospital of Gansu Province, Lanzhou 730050, China

Abstract

Objective The aim of the study was to investigate the effect of parathyroid hormone (PTH) on the apoptosis of human medullary thyroid carcinoma (MTC) cells.

Methods *In vitro* cultured medullary thyroid carcinoma cell lines were treated with parathyroid hormone and parathyroid hormone receptor-monoclonal antibody, and the apoptosis of cells was detected by flow cytometry.

Results The cell morphology changed significantly after treatment based on the observation using the inverted phase-contrast microscope. Various concentrations of parathyroid hormone and parathyroid hormone receptor-monoclonal antibody effectively induced apoptosis in a time- and concentration-dependent manner. When the concentration of parathyroid hormone was 2.0 $\mu\text{mol/L}$ and that of parathyroid hormone receptor-monoclonal antibody was 1.0 $\mu\text{mol/L}$, the apoptotic rate was 13.24% and 20.78%, respectively, representing a statistically significant difference from that of the control cells ($P < 0.05$).

Conclusion PTH plays a role in inducing apoptosis of human MTC cells.

Key words: parathyroid hormone (PTH); medullary thyroid carcinoma (MTC); cell apoptosis

Received: 2 May 2017
Revised: 7 November 2017
Accepted: 20 November 2017

Parathyroid hormone (PTH) is secreted by the parathyroid, and along with calcitonin it regulates calcium and phosphorus metabolism [1]. PTH and its related peptides have been reported to have a proliferative effect on tumor cells [2–3]. In this study, the human medullary thyroid carcinoma (MTC) cell line TT was treated with PTH and anti-PTH receptor antibody (anti-PTHR1), respectively. The growth status of TT cells was observed and the apoptosis rate was measured. These findings on the effect of PTH and anti-PTHR1 on the apoptosis of MTC cells will provide a new theoretical basis for the treatment of MTC.

Materials and methods

Major reagents and equipments

The human MTC cell line TT was obtained from the Shanghai Institute of the Chinese Academy of Sciences (Shanghai, China), F12K medium was obtained from Gibco (USA), and fetal bovine serum, trypsin, ethylenediaminetetraacetic acid, dimethyl sulfoxide, and PTH were purchased from Sigma (St. Louis, MO, USA).

Anti-PTHR1 was obtained from Abcam (Cambridge, MA, USA), the flow cytometry kit was purchased from BD (USA), and an Olympus (Tokyo, Japan) inverted phase-contrast microscope was used. Other conventional equipment and reagents were obtained from domestic companies.

Cell culture and treatment

The human MTC TT cell line was cultured in F12K medium at 37 °C (containing 15% fetal bovine serum, 500 U/mL penicillin, and 100 $\mu\text{g/mL}$ streptomycin) through routine digestion passages. After the logarithmic growth phase of TT cells, three experimental groups were established: (1) control group (without PTH and anti-PTHR1); (2) PTH intervention group; and (3) anti-PTHR1 intervention group. PTH was treated at the various concentrations of 0, 0.5 $\mu\text{mol/L}$, 1.0 $\mu\text{mol/L}$, 1.5 $\mu\text{mol/L}$, and 2.0 $\mu\text{mol/L}$ respectively, and anti-PTHR1 was treated at concentrations of 0, 0.25 $\mu\text{mol/L}$, 0.5 $\mu\text{mol/L}$, 0.75 $\mu\text{mol/L}$, and 1.0 $\mu\text{mol/L}$, respectively. After 48 h, the cells were washed with phosphate-buffered saline (PBS), the supernatant was discarded, and the cells were detected by

✉ Correspondence to: Qinjiang Liu. Email: LIUQJ99@126.com

* Supported by a grant from the Science and Technology Plan Projects of Lanzhou (No. 2013-3-38).

© 2017 Huazhong University of Science and Technology

flow cytometry.

After the cells were cultured for 24 h, the cells in each concentration group were collected, washed with cold PBS, centrifuged, and then the supernatant was discarded. The cell suspension was treated with $1\times$ annexin binding buffer with an average of 10^6 cells in 1 mL of suspension, to a total volume of 100 μ L. Alexa Fluor 488 annexin V (5 μ L) and 1 μ L propidium iodide reserve liquid (100 μ g/mL) were added to the 100- μ L cell suspension. The cells were cultured for 15 min at room temperature and then 400 μ L of $1\times$ annexin-binding buffer was added, and the sample was gently mixed on the ice and tested as soon as possible.

Statistical analysis

SPSS 17.0 software was used for statistical analysis. Data between two groups were compared using *t*-tests, and those among groups were compared using analysis of variance; $P < 0.05$ was considered to indicate a statistically significant difference.

Results

Under the microscope, the cells of the control group were distributed as a monolayer, showing good growth; the cells were transparent and the boundaries were clear. After treatment with PTH and anti-PTHR1 for 24 h, nuclei concentration was initiated, the nuclear membrane gradually disintegrated, and the chromatin showed a great division with an increase in concentration of PTH and anti-PTHR1, and time. Therefore, these cells demonstrated the hallmark changes that occur during apoptosis.

Flow cytometry demonstrated no significant changes in the control group cells, whereas apoptosis of TT cells was clearly detected under all tested concentrations of PTH and anti-PTHR1. The apoptotic effect increased with an increase in their concentration and with increase in time for a given concentration, indicating time- and concentration-dependent effects. Indeed, the apoptosis rate was positively correlated with concentration and time ($P < 0.05$). When the concentration of PTH was 2.0 μ mol/L, the apoptosis rate of TT cells was significantly increased at 13.24% ($P < 0.05$). When the concentration of anti-PTHR1 was 1.0 μ mol/L, the apoptosis rate of TT cells was significantly increased, at 20.78% ($P < 0.05$) (Fig. 1 and 2).

Discussion

MTC is a malignant tumor originating from follicular side cells (C cells), and calcitonin is a specific marker of MTC cells [4-5]. Surgical resection is still the preferred radical approach for treatment. MTC is distinct from

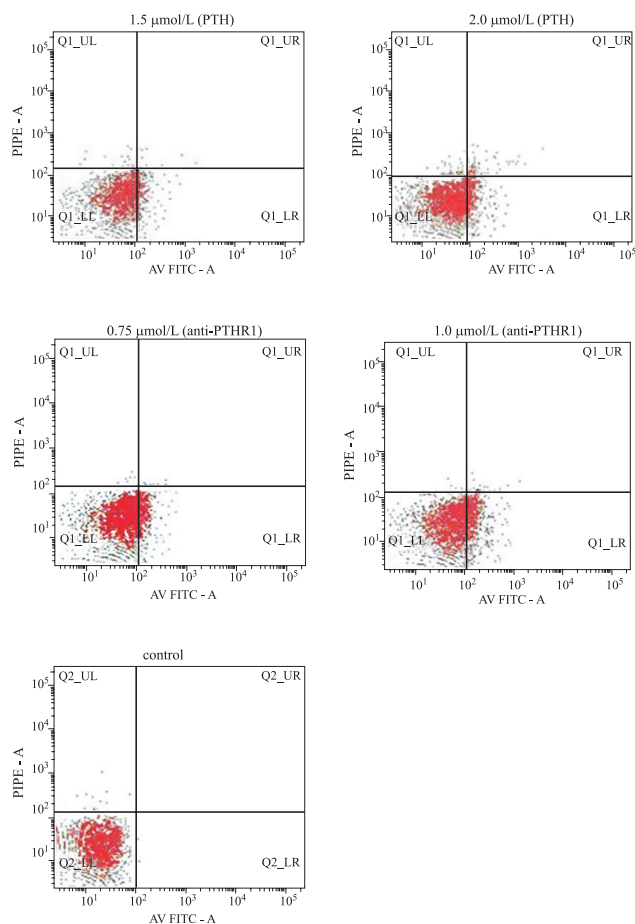


Fig. 1 Apoptosis of TT cells exposed to different concentrations of PTH and anti-PTHR1.

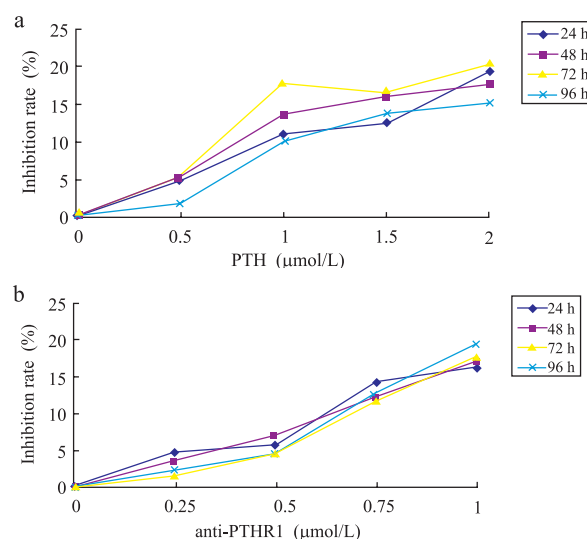


Fig. 2 Inhibitory effects of (a) PTH and (b) anti-PTHR1 on TT cells over time and at different concentrations

differentiated thyroid cancer, as it originates from C cells, it is not affected by thyroid stimulating hormone (TSH), and it does not express sodium/iodide symporter (NIS); therefore, TSH inhibitory therapy and I^{131} radionuclide irradiation treatment is ineffective for MTC, and the 10-year survival rate is much lower than that of patients with differentiated thyroid cancer [6-8]. To date, a variety of immunotherapy strategies, molecular targeted drugs, and tumor vaccines have shown some good effects in preclinical tests; although some of these drugs have started to be used clinically, the therapeutic effect is still not ideal [9-11]. Therefore, the search for new effective molecular therapeutic targets for MTC remains one of the most difficult and hot issues in the field of thyroid cancer research. Thus, further study of the MTC development mechanism and tumor cell growth can help to provide major breakthroughs for developing new therapeutic drugs.

PTH is an endocrine hormone that regulates calcium and phosphorus metabolism. However, its involvement in the development of MTC and its effect on the growth and proliferation of MTC cells have not been reported. Dexamethasone was shown to inhibit the proliferation of TT cells, mainly by inhibiting the G1 phase of the cell cycle to induce apoptosis [12]. Further studies have shown that protein kinase C (PKC) inhibits the proliferation of MTC cells by increasing apoptosis rate *in vitro* [13]. PTH receptor (PTHR) is a member of the G protein-coupled receptor (GPCR) family. After PTH activates the receptor, G protein decomposes into the α , β , and γ subunits, including the Gs, Gi, Gq, and G12/13 subunit, with different signal transduction functions. The Gs and Gi α subunits respectively activate and inhibit adenylate cyclase (AC), and affect cAMP generation and protein kinase A activity. PLC-independent PKC activation pathways (PTH/non-PLC/PKC). Among the above pathways, cAMP/PKA and PLC are the main signaling pathways that mediate the biological effects of PTH. PTHR is expressed in the normal thyroid C membrane surface, and it shows higher expression in MTC. PTHR activates AC by GPCR, enables a higher concentration of cAMP in cells, which activates PKA to initiate the AC-cAMP-PKA pathways. However, there has been no in-depth study on how these signaling pathways are regulated in MTC or on the correlation among the proliferation, apoptosis, and pathogenesis of MTC [14].

In this study, TT cells were treated with PTH and anti-PTHR1, and light microscopy revealed that TT cells were distributed as a monolayer, in spindle or polygonal shape, the cell contour was clear, the cell morphology was complete, and the cells were well grown. After treatment with PTH and anti-PTHR1, the nuclei appeared to be concentrated, marginalized, and the nuclear membrane gradually disintegrated. The chromatin was divided into

several blocks. The apoptosis of the cells was increased with an increase of the drug concentration and with the increase in treatment time. The results of flow cytometry confirmed that all concentrations of PTH and anti-PTHR1 could induce the apoptosis of TT cells, and the difference was significant ($P < 0.05$) compared to the control. The apoptotic rate was positively correlated with concentration and time ($P < 0.05$). The apoptosis of TT cells was most significant when the PTH concentration was 2.0 $\mu\text{mol/L}$ and that of anti-PTHR1 was 1.0 $\mu\text{mol/L}$. These results suggested that PTH and anti-PTHR1 can inhibit the growth of TT cells and play important roles in the induction of apoptosis in a concentration- and time-dependent manner. Some studies have shown that the addition of exogenous PTH1-34 can promote PTH formation in TT cells, induce and activate PTHR1, increase the cAMP level of TT cells, activated the AC-cAMP-PKA pathway, inhibits the growth of TT cells, and ultimately promotes apoptosis. These results are consistent with those of our study.

The effects of PTH and anti-PTHR on the morphology and structure of human MTC TT cells are consistent with cell apoptosis. These results suggest that PTH and anti-PTHR1 have a dual biological effect by inhibiting the proliferation and inducing apoptosis of human MTC TT cells. These findings provide a theoretical basis and important reference for further studies of the mechanism of PTH on MTC.

In summary, this study confirmed that PTH and anti-PTHR1 can effectively induce the apoptosis of human MTC TT cells. This result provides very important information and presents a practical application value for exploring the mechanism of apoptosis induction and the role of PTH on human MTC TT cells. With further in-depth research and understanding of PTH, PTH and anti-PTHR1 may become new anti-tumor therapy targets, providing a new strategy for the early diagnosis and treatment of MTC.

Conflict of interest

The authors indicated no potential conflicts of interest.

References

1. Di Cosimo C, Metere A, Chiesa C, *et al.* Mediastinal parathyroid adenoma: a case report. *Eur Rev Med Pharmacol Sci*, 2012, 16: 845-847.
2. Liang HS, Xue YM, Zhong YH. Effect of parathyroid hormone-related peptide on the proliferation of insulinoma cell line INS-1. *J Pract Med (Chinese)*, 2010, 26: 1286-1288.
3. Ni YQ, Liu QJ, Ma SH, *et al.* Inhibition effects of parathyroid hormone on human medullary thyroid carcinoma cells. *Chinese-German J Clin Oncol*, 2014, 13: 224-228.
4. Yu GP, Li JC, Branovan D, *et al.* Thyroid cancer incidence and survival in the national cancer institute surveillance, epidemiology,

- and end results race/ethnicity groups. *Thyroid*, 2010, 20: 465–473.
5. Kazaure HS, Roman SA, Sosa JA. Medullary thyroid microcarcinoma: a population-level analysis of 310 patients. *Cancer*, 2012, 118: 620–627.
 6. Xu L, Zhao YP, Wang WB, *et al.* Clinical characteristics of hereditary and sporadic medullary thyroid carcinoma. *Acta Acad Med Sin (Chinese)*, 2012, 34: 401–404.
 7. Tian YX, Liu QJ, Ni YQ. Radiofrequency induction on sodium/iodide symporter expression of thyroid cancer. *Chinese–German J Clin Oncol*, 2013, 12: 516–520.
 8. Dionigi G, Tanda ML, Piantanida E. Medullary thyroid carcinoma: surgical treatment advances. *Curr Opin Otolaryngol Head Neck Surg*, 2008, 16: 158–162.
 9. Robinson BG, Paz-Ares L, Krebs A, *et al.* Vandetanib (100 mg) in patients with locally advanced or metastatic hereditary medullary thyroid cancer. *J Clin Endocrinol Metab*, 2010, 95: 2664–2671.
 10. Kurzrock R, Sherman SI, Ball DW, *et al.* Activity of XL184 (Cabozantinib), an oral tyrosine kinase inhibitor, in patients with medullary thyroid cancer. *J Clin Oncol*, 2011, 29: 2660–2666.
 11. Sherman SI. Targeted therapy of thyroid cancer. *Biochem Pharmacol*, 2010, 80: 592–601.
 12. Chung YJ, Lee JI, Chong S, *et al.* Anti-proliferative effect and action mechanism of dexamethasone in human medullary thyroid cancer cell line. *Endocr Res*, 2011, 36: 149–157.
 13. Molè D, Gentilin E, Gagliano T, *et al.* Protein kinase C: a putative new target for the control of human medullary thyroid carcinoma cell proliferation *in vitro*. *Endocrinology*, 2012, 153: 2088–2098.
 14. Gensure RC, Gardella TJ, Jüppner H. Parathyroid hormone and parathyroid hormone-related peptide, and their receptors. *Biochem Biophys Res Commun*, 2005, 328: 666–678.

DOI 10.1007/s10330-017-0227-7

Cite this article as: Hou XF, Liu QJ, Tian YX. Effect of parathyroid hormone on apoptosis of human medullary thyroid carcinoma cells. *Oncol Transl Med*, 2017, 3: 241–244.

Clinical predictive values of biomarker levels in non-small cell lung cancer

Wenqing Wei (✉)

Department of Central Laboratory, Army General Hospital, Beijing 100700, China

Abstract

Objective To evaluate the predictive value of serum levels of PD-1, IL-17, and IL-21 in patients with non-small cell lung cancer.

Methods Serum levels of PD-1, IL-17, and IL-21 were analyzed by ELISA in 45 patients with non-small cell lung cancer (NSCLC) and 30 healthy individuals.

Results Serum PD-1, IL-17, and IL-21 levels were significantly different between preoperative patients with NSCLC and the control group ($P < 0.01$), while there was no significant differences between the postoperative patients and the control group ($P > 0.05$). Comparison of serum PD-1, IL-17, and IL-21 levels of patients with NSCLC before and after the operation revealed a decrease in PD-1 and IL-17 levels and an increase in IL-21 levels. The serum levels of PD-1 and IL-17 were higher in patients with advanced staged disease than in those with early stage cancer ($P < 0.05$), while IL-21 levels were lower at the advanced stages ($P < 0.05$).

Conclusion In patients with NSCLC, serum levels of PD-1, IL-17, and IL-21 changed considering the surgical operation and the course of the disease. Screening these biomarker levels might provide a helpful index for treatment and prognosis

Keywords: non-small cell lung cancer; PD-1; IL-17; IL-21

Received: 18 July 2017
Revised: 23 August 2017
Accepted: 27 September 2017

Lung cancer is a malignant disease with rapid recurrence and high mortality rates^[1], and is the most common cause of death among patients with cancer in China. More than 85% of patients with lung cancer present with non-small cell lung cancer (NSCLC), which has a 5-year survival rate of only about 15%^[2]. Studies have identified a variety of immune molecules involved in the occurrence and development of NSCLC, and detecting the related immune molecules might be helpful for early diagnosis, effective treatment, and improving the prognosis of the disease. The programmed cell death protein 1 (PD-1) was isolated in 1992 and belongs to the B7 family of immunoglobulins. PD-1 is an important negative costimulatory molecule that, upon binding to its ligand, inhibits T cell activation, proliferation, participation in immune tolerance, and immune evasion, which promote tumor development and progression. Interleukin-21 (IL-21) is a type I cytokine that was discovered by Parrish-Novak in 2000 and plays an important role in anti-tumor and anti-virus immune functions by promoting the activation, proliferation, and differentiation of NK, B, and T cells. The role of IL-21 in

the development, progression, and metastasis of NSCLC has not yet been elucidated^[3–4]. Interleukin 17 (IL-17) is a proinflammatory cytokine that stimulates epithelial cells, endothelial cells, and fibroblasts to produce a variety of cytokines that induce inflammation^[5–8]. IL-17 has been found to induce tumor angiogenesis and promote tumor growth, invasion, and metastasis in NSCLC animal models. In this study, we investigated PD-1, IL-21, and IL-17 levels in the peripheral blood of patients with NSCLC and healthy individuals to explore the significance of these potential biomarkers in the development and progression of NSCLC.

Materials and methods

Materials

From January 2015 to December 2016, 45 inpatients diagnosed with primary non-small cell lung cancer were recruited for our study. This patient cohort included 25 men and 20 women, with an average age of 56.1 years (range, 38 to 70 years). The normal control group

included 30 healthy volunteers, 14 men and 16 women, and the average age was 53.4 years (range, 36 to 65 years). All patients provided informed consent and reported to the hospital ethics committee for approval. Patient were diagnosed through tissue biopsy, fiberoptic bronchoscopy, and/or chest computed tomography. Diagnostic criteria were categorized in reference to the WHO classification of lung cancer histological criteria [9], and the patients with NSCLC were divided into 21 patients with squamous cell carcinoma and 24 patients with adenocarcinoma. Postoperative pathological stage was determined by TNM standardization (International Union Against Cancer Classification in 2002), and the patients were classified as 7 patients with stage I, 11 patients with stage 2, 17 patients with stage 3, and 10 patients with stage 4 cancer.

Instruments and reagents

IL-17 and IL-21 ELISA kits were purchased from Beijing Jingmei Bioengineering Co., Ltd. The PD-1 ELISA kit was purchased from R&D Systems, USA.

PD-1, IL-17, and IL-21 quantification with ELISA

Venous blood (4 mL) from patients was drawn 3 days before and 7 days after the operation. The blood was made to stand for 1 h at room temperature and was centrifuged at 2500 r/min for 15 min. PD-1, IL-17, and IL-21 were measured by using double antibody sandwich ELISA. According to manufacturer instructions, each sample and standard was repeated three times.

Statistical analysis

The data were expressed as mean \pm standard deviation (mean \pm SD). Statistical comparisons, using analysis of variance, were performed with SPSS 13.0 software. *P* values less than 0.05 were considered statistically significant.

Results

The levels of serum PD-1, IL-17, and IL-21 in patients with NSCLC and healthy subjects, determined by ELISA

Serum levels of PD-1, IL-17, and IL-21 in 45 patients with NSCLC were significantly different from those of healthy volunteers ($P < 0.01$) (Table 1). Serum IL-21 levels were significantly greater ($P < 0.05$), and serum PD-1 and IL-17 levels were significantly lower, than those observed in the postoperative group ($P < 0.05$).

The relationship between the serum levels of PD-1, IL-17, and IL-21 in patients with NSCLC and corresponding clinicopathological features

The levels of serum PD-1 and IL-17 gradually increased with TNM stage progression, and the differences were significant ($P = 0.031$, $P = 0.037$). IL-21 levels decreased gradually as the TNM stage progressed, and this difference was significant ($P = 0.025$). The changes in serum PD-1, IL-17, and IL-21 levels did not correlate with the pathological type of NSCLC. There were no significant differences in the levels of squamous cell carcinoma and adenocarcinoma between the two groups ($P = 0.249$, $P = 0.251$, $P = 0.305$; Table 2).

The relationship between PD-1, IL-17, and IL-21 levels in patients with NSCLC

There was a negative correlation between PD-1 and IL-21 levels in the peripheral blood of patients with NSCLC ($r = 0.031$, $P = 0.532$) and between IL-17 and IL-21 levels ($r = 0.012$, $P = 0.325$). There was a positive correlation between PD-1 and IL-21 levels in the peripheral blood of patients with NSCLC ($r = 0.534$, $P = 0.265$).

Discussion

As NSCLC does not usually show early clinical manifestations, most patients with NSCLC are diagnosed in the advanced stage. At the time of NSCLC diagnosis, tumor cells already exhibit invasion and metastasis, which affect disease treatment and prognosis, thereby underscoring the need to monitor and control tumor cell

Table 1 The serum levels of IL-17, IL-21 and PD-1 of the preoperative and postoperative NSCLC patients vs controls ($\bar{x} \pm s$)

Group	n	IL-17 (pg/mL)		IL-21 (pg/mL)		PD-1 (pg/mL)	
		Pre-operate	Post-operate	Pre-operate	Post-operate	Pre-operate	Post-operate
NSCLC	45	46.21 \pm 13.42	26.89 \pm 8.13	63.21 \pm 12.21	82.46 \pm 10.87	110.34 \pm 20.13	55.27 \pm 14.76
Control	30	20.08 \pm 7.93	–	86.93 \pm 10.62	–	51.22 \pm 15.12	–
<i>t</i>		3.679	1.693	3.435	1.652	4.009	1.730
<i>P</i>		0.031	0.093	0.042	0.102	0.020	0.134

Table 2 The relationship between the serum level of PD-1, IL-17, IL-21 of NSCLC patients and clinical pathological features ($\chi \pm s$)

Clinical pathological features	n	IL-17		IL-21		PD-1	
		pg/mL	P	pg/mL	P	pg/mL	P
TNM staging							
Stage I	7	37.56 ± 4.33	0.037	78.36 ± 11.49	0.025	92.14 ± 17.22	0.031
Stage II	11	46.64 ± 5.61		67.74 ± 10.02		102.47 ± 22.53	
Stage III	17	54.71 ± 6.19		57.13 ± 10.87		115.35 ± 20.98	
Stage IV	10	62.59 ± 6.85		48.32 ± 9.62		128.31 ± 22.34	
Pathological type							
Squamous cell	21	51.81 ± 5.46	0.251	66.67 ± 12.81	0.305	109.14 ± 19.73	0.249
Carcinoma adenocarcinoma	24	53.34 ± 5.78		61.32 ± 14.34		115.25 ± 21.82	

metastasis for patients with NSCLC [10].

The development of NSCLC is closely related to immune status and function. T lymphocytes play an important role in cellular immunity, and CD4+ T cells participate in the immune response at all stages. Th17 cells belong to a CD4+ T cell subset and secrete IL-17 and other cytokines involved in tumor development. In NSCLC mouse models, IL-17 has been found to induce the migration of vascular endothelial cells and formation of endothelial cells, promote the secretion of cytokines such as VEGF, TGF- β 1 and PGE2 in tumor or tumor stromal cells, and promote tumor growth, metastasis, and infiltration. IL-21 is a type I cytokine that is secreted by activated CD4+ T cells and NKT cells and contains a chain that is in common with IL-2, IL-4, and IL-15 cytokines. IL-21 can promote lymphocyte proliferation and differentiation and enhance the cytotoxicity of CD8+ T and NK cells. The regulation of IL-21 on immune cells is bidirectional, and depends on microenvironmental factors such as synergistic cytokines [11–13].

The immune escape of tumor cells is closely related to the abnormal expression of synergistic molecules. PD-1/PD-L1 is an important member of the B7/CD28 costimulatory molecule superfamily and has been shown to be responsible for the regulation of T cells by suppressing T cell activation and proliferation, which results in the immune escape of tumor cells. The PD-1 pathway has become a new hotspot for cancer therapy [14–15].

In this study, we measured serum PD-1, IL-17, and IL-21 levels in 45 patients with NSCLC. In comparison with 30 healthy volunteers, the levels of PD-1 and IL-17 in the peripheral blood of patients with NSCLC increased, and IL-21 levels decreased. We hypothesize that these three immune molecules might be involved in the occurrence of NSCLC, and for further investigation, we compared the changes in serum levels of these cytokines in patients before and after surgery. After treatment, the serum levels of IL-17 and PD-1 decreased and IL-21 increased, which are closely associated with tumor load. In order to elucidate whether PD-1, IL-17, and IL-21 levels have

a certain relationship with NSCLC pathological stage, serum levels of 45 patients with NSCLC were analyzed according to TNM staging. The results showed that serum PD-1 and IL-17 levels increased with the progression of NSCLC ($P = 0.031$, $P = 0.037$), suggesting that PD-1 and IL-17 were involved in the proliferation, infiltration, and metastasis of NSCLC. The level of IL-21 decreased gradually as TNM stage progressed ($P = 0.025$), suggesting that as the clinical stage of NSCLC progresses, the immune function of gradually reduces and IL-21 level decreases. Our experimental data showed that there were no significant differences in serum PD-1, IL-17, and IL-21 levels between patients with squamous cell carcinoma and those with adenocarcinoma, suggesting that serum levels of PD-1, IL-17, and IL-21 were not related to the pathological subtype of NSCLC.

In summary, the results of our study show that changes in serum PD-1, IL-17, and IL-21 levels in patients with NSCLC are associated with the development, progression, and metastasis of NSCLC. Monitoring the levels of PD-1, IL-17, and IL-21 may be important for guiding the treatment and prognosis of patients with NSCLC.

Conflict of interest

The authors indicated no potential conflicts of interest.

References

1. Torre LA, Bray F, Siegel RL, *et al.* Global cancer statistics, 2012. *CA Cancer J Clin*, 2015, 65: 87–108.
2. Chen W, Zheng R, Zeng H, *et al.* Annual report on status of cancer in China, 2011. *Chin J Cancer Res*, 2015, 27: 2–12.
3. Ishida Y, Agata Y, Shibahara K, *et al.* Induced expression of PD-1, a novel member of the immunoglobulin gene superfamily, upon programmed cell death. *EMBO J*, 1992, 11: 3887–3895.
4. Shien K, Papadimitrakopoulou VA, Wistuba II, *et al.* Predictive biomarkers of response to PD-1/PD-L1 immune checkpoint inhibitors in non-small cell lung cancer. *Lung Cancer*, 2016, 99: 79–87.
5. Parrish-Novak J, Dillon SR, Nelson A, *et al.* Interleukin 21 and its receptor are involved in NK cell expansion and regulation of lymphocyte function. *Nature*, 2000, 408: 57–63.
6. Denman CJ, Senyukov W, Somanchi SS, *et al.* Membrane-bound IL-

- 21 promotes sustained *ex vivo* proliferation of human natural killer cells. *PLoS One*, 2012, 7: e30264.
7. Harrington LE, Hatton RD, Mangan PR, *et al.* Interleukin 17-producing CD4+ effector T cells develop via a lineage distinct from the T helper type 1 and 2 lineages. *Nat Immunol*, 2005, 6: 1123–1132.
 8. Numasaki M, Watanabe M, Suzuki T, *et al.* IL-17 enhances the net angiogenic activity and *in vivo* growth of human non-small cell lung cancer in SCID mice through promoting CXCR-2-dependent angiogenesis. *J Immunol*, 2005, 175: 6177–6189.
 9. Beasley MB, Brambilla E, Travis WD. The 2004 World Health Organization classification of lung tumors. *Semin Roentgenol*, 2005, 40: 90–97.
 10. Molina JR, Yang P, Cassivi SD, *et al.* Non-small cell lung cancer: epidemiology, risk factors, treatment, and survivorship. *Mayo Clin Proc*, 2008, 83: 584–594.
 11. Xu C, Yu L, Zhan P, *et al.* Elevated pleural effusion IL-17 is a diagnostic marker and outcome predictor in lung cancer patients. *Eur J Med Res*, 2014, 19: 23.
 12. Si LB, Tian H, Qi L, *et al.* Detection of Th17 in peripheral blood of patients with primary non-small cell lung cancer and its clinical significance. *Chin J Gerontol (Chinese)*, 2014, 34: 6049–6051.
 13. Spolski R, Leonard WJ. Interleukin-21: a double-edged sword with therapeutic potential. *Nat Rev Drug Discov*, 2014, 13: 379–395.
 14. Shi LX, Li L, Guo L, *et al.* PD-1 and PD-L1 treatment of non-small cell lung cancer clinical research status. *Cancer Prog (Chinese)*, 2017, 15: 4–6.
 15. Wang WL, Liao P, Xu PB, *et al.* Advances in the strategy of individualized drug use in tumor immunodeficiency syndrome. *Chin J Clin Pharmacol Ther (Chinese)*, 2017, 22: 228–232.

DOI 10.1007/s10330-017-0236-6

Cite this article as: Wei WQ. Clinical predictive values of biomarker levels in non-small cell lung cancer. *Oncol Transl Med*, 2017, 3: 245–248.

Function and clinical significance of SUMOylation in type I endometrial carcinoma

Xin Cui^{1, 2}, Caixin Zhang², Yunhui Li³, Yongyun Qi¹, Xiaoyan Ding⁴, Shumin Hei¹, Weiqing Huang²(✉)

¹ Department of Pathology, The Third Affiliated Hospital of Qingdao University, Qingdao 266000, China

² Department of Pathology, Qingdao Municipal Hospital, Qingdao 266000, China

³ Department of Obstetrics and Gynecology, The Affiliated Medical College of Qingdao University, Qingdao 266100, China

⁴ Department of Pathology, The Affiliated medical college of Qingdao University, Qingdao 266100, China

Abstract

Objective This study elucidated the function and role of SUMOylation in type I endometrial carcinoma.

Methods Fifty type I endometrial carcinoma cases and para-cancer tissue samples were collected. The expression levels of ubiquitin-conjugating enzyme E2 I (Ube2i, Ubc9) and small ubiquitin-like modifier 1 (SUMO1)/sentrin-specific peptidase 1 (SEN1) proteins were examined using immunohistochemistry and the correlation with clinicopathological parameters was analyzed.

Results Ubc9 expression in type I endometrial carcinoma tissues was significantly higher than that in the para-cancer tissues; in contrast, the expression of the SEN1 protein was markedly lower than that in the para-cancer tissues. Ubc9 and SEN1 expression levels were negatively correlated and were associated with tumor differentiation, but not age, depth of invasion, tumor stage, and lymph node metastasis.

Conclusion SUMOylation modification plays a major role in the pathogenesis and development of type I endometrial carcinoma. Thus, it could be a potential target for the treatment of endometrial cancer.

Keywords SUMOylation; Ubc9; sentrin-specific peptidase 1 (SEN1); immunohistochemistry

Received: 16 June 2017
Revised: 23 August 2017
Accepted: 27 September 2017

Endometrial carcinoma, a malignant epithelial tumor that primarily occurs in perimenopausal and postmenopausal women, is becoming one of the most common tumors of the female reproductive system. Furthermore, it is the third most common gynecological malignancy leading to death (underlying ovarian and cervical cancers). Histologically, endometrial carcinoma is classified as type I and II. Accounting for 90% of endometrial carcinomas, type I is a low-grade tumor associated with estrogen. Recent studies have shown the involvement of gene alterations including in phosphatase and tensin homolog (*PTEN*) and *KRAS* proto-oncogene, GTPase (*K-RAS*) as well as microsatellite instability in the pathogenesis of carcinoma. However, the underlying molecular mechanisms are unknown.

Small ubiquitin-like modifier (SUMO), which is a highly conserved protein is expressed as a small ubiquitin-

related modification in eukaryotes [1] and regulates the function of target proteins by SUMOylation. This modification is mainly mediated by covalent binding with substrate proteins. The SUMOylation process requires the actions of the E1-activating and E2-conjugating enzymes and E3 ligases [2]. Previous studies have demonstrated that the only ubiquitin-conjugating enzyme, E2 I (Ube2i, Ubc9), plays a key role in the development of tumors [3]. SUMOylation is a dynamic and reversible process, and the SUMO-substrate combination can be separated by specific enzymes. Previous studies identified the expression of SUMO-specific proteases (SENPs), which are responsible for separating SUMO and its target proteins, in various tumor tissues and showed their participation in the pathophysiology of tumor development [4-6]. Studies found that SENP1 expression was significantly elevated in prostate, gastric, and breast cancer tissues

[7-9]; however, no related reports on its expression and function in endometrial carcinoma are available. Thus, our prospective study used immunohistochemical staining to detect the differential expression of Ubc9 and SENP1 proteins in type I endometrial cancer tissues to evaluate the role of SUMO modification in ontogenesis and development of type I endometrial carcinoma.

Materials and methods

Clinical data

Specimens from 50 patients with type I endometrial carcinoma and adjacent normal tissues were collected randomly after surgical resection in the patients at the Qingdao Municipal Hospital. The samples were confirmed by postoperative pathological diagnosis. These included 9, 16, and 25 cases with high, moderate, and low differentiation, respectively. The range and median age of the patients was 42–70 and 56 years, respectively, consisting of 14 and 36 patients who were < 50 and ≥ 50 years old, respectively. According to the 2009 International Federation of Gynecology and Obstetrics (FIGO) staging method, 21, 20, 9, and 0, patients were in stages I, II, III, and IV, respectively, whereas 23 and 27 patients showed the presence and absence of lymph node metastasis, respectively.

Reagents

Rabbit anti-human SENP1 and anti-human Ubc9 antibodies (Abcam, UK), enzyme-labeled sheep anti-mouse/rabbit IgG polymer (Zhongshan Company, Beijing), animal serum (sheep, Maixin Biotechnology Co., Ltd., China), and 3% hydrogen peroxide (Maixin Biotechnology Co., Ltd., China) were used in this study.

Test methods

The specimens were fixed for 24 h in 10% formalin, embedded in paraffin, and sliced into 6 μm thick sections, followed by xylene dewaxing, gradient alcohol dehydration, high-pressure repair, 3% hydrogen peroxide-based removal of endogenous enzymes, blocking with animal serum (sheep), and incubation with primary antibodies: rabbit anti-human SENP1 polyclonal antibody (1:400) and rabbit anti-human Ubc9 antibody (1:1000). Subsequently, the secondary antibody, enzyme-labeled goat anti-mouse anti-rabbit IgG/polymer was added, followed by 3, 3'-diaminobenzidine (DAB) staining, hematoxylin counterstaining, acid alcohol differentiation, dehydration, transparency treatment, sealing with a neutral gum piece, and microscopic

examination. The testicular tissue was used as a positive control (according to the instructions from the SENP1 antibody manufacturer). Phosphate-buffered saline (PBS) was used as a negative control instead of the primary antibody.

Determination standard

The determination standard used was that proposed in the method of Liang *et al* [10], which specifies to observe the specimen 200 times under an optical microscope. Cells with distinct brown granules were considered positive. The Ubc9 protein was positively expressed primarily in the cytoplasm of the tumor and stromal cells and brown granules with different thicknesses and depths were also observed. The SENP1 protein was mainly positively expressed in the nucleus. Each tissue slice was randomly examined in 10 high-power visual fields and evaluated based on the depth of the cell color using a point scale that was divided into four grades: no color, 0 points; weak, 1 point; medium, 2 points; and strong, 3 points. The following percentages of positive tumor cells were assigned to the four grades: ≤10%, >10–30%, >30–60%, >60% to 0, 1, 2, and 3 points, respectively. The final result was the sum of two phases: 0-1 point, “-”; 2-3 points, “+”; 4-5 points, “++”; 6 points, “+++.” The double-blind method was used to determine the final result, and each slice was assessed by two pathologists and re-enumerated when the difference was >10%.

Statistical analysis

The statistical package for the social sciences (SPSS) version 16 software was used to analyze the data using the Chi-squared (χ^2) test. Fisher's probability and Spearman's methods were used for the correlation analysis and a $P < 0.05$ was considered statistically significant.

Results

Expression of SENP1 protein in endometrial carcinoma and adjacent normal tissues

The Ubc9 protein was primarily expressed in the tumor and adjacent tissues. However, the positive expression level was significantly lower in the adjacent normal tissues [18% (9/50)] than it was in the tumor tissues [84% (42/50)]. In contrast, the positive Ubc9 expression level in the endometrial carcinoma tissue was significantly higher than that in the adjacent normal tissue was ($P < 0.001$, Table 1 and Fig 1).

Expression of SENP1 protein in endometrial carcinoma and adjacent normal tissues

The SENP1 protein was primarily positively expressed in the adjacent normal and tumor tissues. However, the positive expression level was significantly lower in tumor tissues at 54% (27/50) than it was in the adjacent normal tissues at 100% (50/50). Thus, the positive SENP1 expression level in endometrial carcinoma was significantly lower than that in the adjacent normal tissue ($P < 0.001$, Table 2 and Fig 2).

Relationship between Ubc9 protein expression and clinicopathological features

The analysis of the relationship between Ubc9 protein expression and clinicopathological features showed that the expression was related to the degree of tumor differentiation ($P < 0.05$). However, no correlation was established with the patients' age, depth of invasion, FIGO stage, and lymph node metastasis ($P > 0.05$, Table 3 and Fig 1).

Table 1 Expression of Ubc9 protein in endometrial carcinoma and adjacent normal tissues (n)

Group	Case	Ubc9				χ^2 value	P-value
		-	+	++	+++		
Carcinoma	50	8	9	11	22		
Adjacent tissues	50	41	6	2	1	48.22	< 0.001

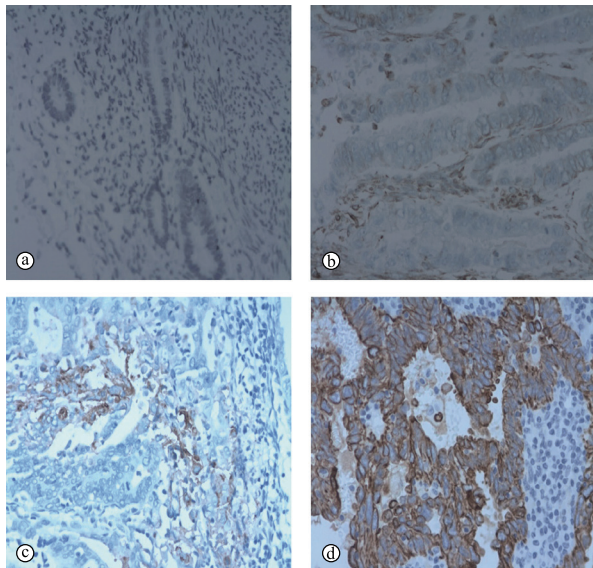


Fig. 1 Expression of Ubc9 in type I endometrial carcinoma and its adjacent tissues (HE, $\times 200$). (a) adjacent tissues,Ubc9 was low expression. (b) high differentiation tumor tissues,Ubc9 was also low expression, but was higher than in (a). (c)middle differentiation tumor tissues,Ubc9 was middle expression; (d) low differentiation tumor tissues, Ubc9 was high expression

Table 2 Expression of SENP1 protein in endometrial carcinoma and adjacent normal tissues (n)

Group	Case	SENP1				χ^2 value	P-value
		-	+	++	+++		
Carcinoma	50	23	3	6	18		
Adjacent tissues	50	0	5	7	38	30.72	< 0.001

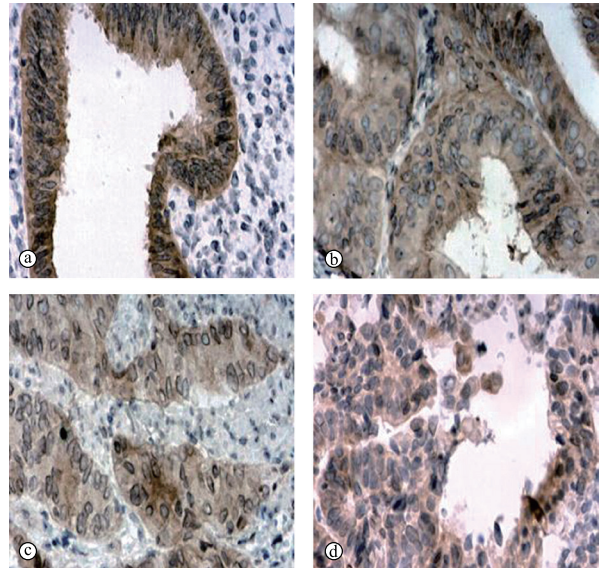


Fig. 2 Expression of SENP1 in type I endometrial carcinoma and its adjacent tissues (HE, $\times 200$) (a) adjacent tissues, SENP1 was high expression. (b) high differentiation tumor tissues,SENP1 was also high expression, but was higher than in (a). (c) middle differentiation tumor tissues, SENP1 was middle expression. (d) low differentiation tumor tissues, SENP1 was low expression)

Table 3 Relationship between Ubc9 protein expression and clinical pathological features (n)

Group	Case	Ubc9				P-value
		-	+	++	+++	
Age (years)						
< 50	14	1	2	5	6	
≥ 50	36	7	7	6	16	0.425
Depth of invasion						
< 1/2 muscle layer	19	3	4	6	6	
$\geq 1/2$ muscle layer	31	5	5	5	16	0.472
Lymph node metastasis						
Yes	27	4	4	7	12	
No	23	4	5	4	10	0.849
Tumor degree						
Low	25	1	4	8	12	
Middle	16	2	3	2	9	
High	9	5	2	1	1	0.021
FIGO Stage						
I	21	4	5	5	7	
II	20	3	3	4	10	
III	9	1	1	2	5	0.912

Table 4 Relationship between SENP1 protein expression and clinical pathological features

Group	Case	SENP1				P-value
		-	+	++	+++	
Age (years)						
< 50	14	7	2	3	2	0.096
≥ 50	36	16	1	3	16	
Depth of invasion						
< 1/2 muscle layer	19	8	1	2	8	0.919
≥ 1/2 muscle layer	31	15	2	4	10	
Lymph node metastasis						
Yes	27	12	2	4	9	0.863
No	23	11	1	2	9	
Tumor degree						
Low	25	18	1	3	3	0.003
Middle	16	4	2	2	8	
High	9	1	0	1	7	
FIGO Stage						
I	21	9	0	2	10	0.292
II	20	8	2	3	7	
III	9	6	1	1	0	

Table 5 Correlation between Ubc9 and SENP1

	Ubc9	SENP1	r value	P-value
-	8	23		
+	9	3		
++	11	6		
+++	22	18		
Total	50	50	-0.20	0.006

Relationship between SENP1 protein expression and clinicopathological characteristics

The analysis of the relationship between SENP1 protein expression and clinicopathological characteristics revealed that the expression of SENP1 was related to the degree of tumor differentiation ($P < 0.05$); however, no association was noted with patient's age, depth of tumor invasion, FIGO stage, and lymph node metastasis ($P > 0.05$, Table 4 and Fig 2).

Correlation between Ubc9 and SENP1

The Spearman's analysis showed that the expression of Ubc9 was negatively correlated with that of SENP1 ($P < 0.05$, Table 5).

Discussion

SUMOylation modification is a dynamic and reversible process mediated primarily by activation, binding, and connection, which leads to modification [11]. Although SUMOylation and ubiquitination are similar, SUMOylation is more stable and cannot be degraded easily by a protease compared to ubiquitination [12]. The covalent link between SUMO and its target proteins requires a cascade of enzymes including; Ubc9, which is the only E2 conjugating enzyme and was first discovered in the lower animals [13]. E2 is correlated with cell meiosis and cell cycle regulation [14]. Ubc9 plays a major role in cell cycle and DNA damage repair, and these pathways are directly or indirectly related to tumorigenesis [2]. In the early stage of malignant cell transformation, the expression levels of Ubc9 and SUMO proteins were increased significantly [12]. Recent studies have also shown that Ubc9 is highly expressed in several tumors such as breast, ovarian, and lung cancers [15-16]; however, only a few reports are available about endometrial carcinoma.

The reverse reaction of SUMOylation modification, which separates SUMO and the target proteins, is termed deSUMOylation and this process is primarily mediated by SENPs [17]. SENP1 belongs to the SENP family of proteins and catalyzes the separation of numerous SUMO-target protein combinations. Although the specific mechanism of the action of SENPs in the pathogenesis and development of tumors is unclear, studies have shown that the disruption of SUMOylation balance promotes tumor occurrence and development. SENPs, as critical enzymes in the deSUMOylation process, play a vital role in maintaining the dynamics of SUMOylation [18]. Therefore, further studies on the function of SENPs and the mechanism underlying deSUMOylation would provide insights into the processes that balance SUMOylation modifications and contribute to elucidating the mechanism of tumor occurrence and progression.

Tumor growth requires nutrients and hypoxia, which is one of the factors affecting the supply of nutrients, is mainly mediated by the coordination of the hypoxia-inducible factor (HIF)-1 α [19]. Cheng *et al* [20] reported that knockout of the SENP1 gene could enhance the SUMOylation of HIF-1 α , leading to its α degradation. Therefore, SENP1 gene knockout mice do not survive, which might be attributed to the lack of new blood vessels formation, thereby illustrating the vital role of SENP1 in tumor occurrence and development.

In this study, we used Ubc9 and SENP1 antibodies to examine SUMOylation in type I endometrial carcinoma and adjacent normal tissues. The results showed that the level of positive Ubc9 expression was significantly higher in the tumor tissue than that in the adjacent normal tissues ($P < 0.05$). The positive SENP1 expression level was significantly lower in tumor tissues than that in the adjacent

normal tissues ($P < 0.05$), indicating that SUMOylation considerably affected type I endometrial carcinoma occurrence and development. The present study also found that the expression levels of the two proteins were related to the degree of tumor differentiation ($P < 0.05$). Moreover, Ubc9 and SENP1 were negatively correlated and played a crucial role in the observed SUMOylation and deSUMOylation, respectively. However, whether this function is antagonistic or the proteins interactive with each to maintain the SUMOylation dynamics is yet to be studied. Furthermore, in advanced melanoma, inhibition of Ubc9 expression increases the sensitivity of melanoma to chemotherapy^[21]. Therefore, whether SENP1 can be used to antagonize Ubc9 to improve tissue sensitivity to chemotherapy in endometrial carcinoma should be addressed. An intensive study of the mechanism underlying SUMOylation might identify a target for endometrial carcinoma treatment.

Conflicts of interest

The authors indicated no potential conflicts of interest.

References

- Hannoun Z, Greenhough S, Jaffray E, *et al.* Post-translational modification by SUMO. *Toxicology*, 2010, 278: 288–293.
- Zou Hongyan, Wu Jie, Fu sb. SUMO binding enzyme Ubc9 and tumor research progress. *Int J genet (Chinese)*, 2015, 38: 320–324.
- Qiu JY, Guo WH. UBC9 and cancer research progress. *Chem Life*, 2015, 3: 301–306.
- Burdelsk C, Menan D, Tsourlakis MC, *et al.* The prognostic value of SUMO1/Sentrin specific peptidase 1 (SENP1) in prostate cancer is limited to ERG-fusion positive tumors lacking PTEN deletion. *BMC Cancer*, 2015, 15: 538.
- Bawa-Khleif T, Cheng J, Wang Z, *et al.* Induction of the SUMO-specific protease 1 transcription by the androgen receptor in prostate cancer cells. *J Biol Chem*, 2007, 282: 37341–37349.
- Cheng J, Wang D, Wang Z, *et al.* SENP1 enhances androgen receptor-dependent transcription through desumoylation of histone deacetylase 1. *Mol Cell Biol*, 2004, 24: 6021–6028.
- Wang Q, Xia N, Li T, *et al.* SUMO-specific protease 1 promotes prostate cancer progression and metastasis. *Oncogene*, 2013, 32: 2493–2498.
- Chen J, Gao Q, Shi Y, *et al.* Expression of SENP1 and P53 in gastric carcinoma and its significance. *J Surg Concepts Pract*, 2012, 17: 659–663.
- Chen J, Wang J, Gu HY, *et al.* The clinical significance of expression of SENP1 and CerBb-2 in breast carcinoma. *J Diagn Concepts Pract*, 2009, 8: 175–179.
- Xu LZ, Yang WT. Criteria for judging the immunohistochemistry results. *Chin J Cancer (Chinese)*, 1996, 6: 229–231.
- Dohmen RJ. SUMO protein modification. *Biochim Biophys Acta*, 2004, 1695: 113–131.
- Li H, Wu BG, Niu HY, *et al.* Expression and significance of Ubc9 in lung cancer. *Mod Oncol*, 2014, 10: 2343–2346.
- Lin JY, Ohshima T, Shimotohno K. Association of Ubc9, an E2 ligase for SUMO conjugation, with p53 is regulated by phosphorylation of p53. *FEBS Lett*, 2004, 573: 15–18.
- Jackson SP, Durocher D. Regulation of DNA damage responses by ubiquitin and SUMO. *Mol Cell*, 2013, 49: 795–807.
- Alshareeda AT, Negm OH, Green AR, *et al.* SUMOylation proteins in breast cancer. *Breast Cancer Res treat*, 2014, 144: 519–530.
- Moschos SJ, Mo YY. Role of SUMO/Ubc9 in DNA damage repair and tumorigenesis. *J Mol Histol*, 2006, 37: 309–319.
- Yeh ET, Gong L, Kamitani T. Ubiquitin-like proteins: new wines in new bottles. *Gene*, 2000, 248: 1–14.
- Han L, Wu HJ. Molecular mechanisms of SENPs on regulating tumor development. *Prog Physiol Sci*, 2013, 44: 55–58.
- Cheng JK. SUMO protease 1 and tumor. *Cancer*, 2008, 27: 771–774.
- Cheng J, Kang X, Zhang S, *et al.* SUMO-specific protease 1 is essential for stabilization of HIF1alpha during hypoxia. *Cell*, 2007, 131: 584–595.
- Moschos SJ, Smith AP, Mandic M, *et al.* SAGE and antibody array analysis of melanoma-infiltrated lymph nodes: identification of Ubc9 as an important molecule in advanced-stage melanomas. *Oncogene*, 2007, 26: 4216–4225.

DOI 10.1007/s10330-017-0245-5

Cite this article as: Cui X, Zhang CX, Li YH, *et al.* Function and clinical significance of SUMOylation in type I endometrial carcinoma. *Oncol Transl Med*, 2017, 3: 249–253.

Expression of CXCL12-CXCR4 in osteosarcoma and its correlation with angiogenesis

Lu Han^{1,2}, Yangyang Shen³, Wenhua Zhao⁴, Baoyong Sun⁵, Xin Zhang⁵, Kai Cui²,
Lei Zhou⁵ (✉), Sheng Li^{1,2,6,7} (✉)

¹ School of Medicine and Life Sciences, University of Jinan-Shandong Academy of Medical Sciences, Jinan 250117, China

² Department of Hepatobiliary Surgery, Shandong Academy of Medical Sciences, Shandong Cancer Hospital affiliated to Shandong University, Jinan 250117, China

³ Department of Anesthesiology, Shandong Academy of Medical Sciences, Shandong Cancer Hospital affiliated to Shandong University, Jinan 250117, China

⁴ Department of Tumor Minimally Invasive Surgery, Qianfo Hill Hospital of Shandong Province, Jinan 250014, China

⁵ Department of Bone & Soft Tissue Surgery, Shandong Academy of Medical Sciences, Shandong Cancer Hospital affiliated to Shandong University, Jinan 250117, China

⁶ Shandong Institute of Pharmaceutical Research, Jinan 250062, China

⁷ Shandong Provincial Collaborative Innovation Center for Neurodegenerative Disorders, Qingdao University, Qingdao 266071, China

Abstract

Objective The expression of CXCL12 (stromal cell-derived factor-1)-CXCR4 (chemokine receptors-4) in osteosarcoma and its role in angiogenesis were examined.

Methods The expression of CXCR4 and CXCL12 in 40 cases of osteosarcoma was detected by immunohistochemistry and real-time fluorescence quantitative PCR. The expression of CD34 in osteosarcoma was detected by immunohistochemistry. Morphometric image analysis was performed to measure microvessel density (MVD). Additionally, the relationship between CXCL12 and CXCR4 expression and MVD of osteosarcoma and pulmonary metastasis were analyzed.

Results The positive rates of CXCL12 and CXCR4 protein expression in osteosarcoma were 40.0% (16/40) and 60.0% (24/40), respectively. Fluorescence quantitative real-time PCR indicated that the expression level of CXCR4 mRNA in pulmonary metastatic osteosarcoma was higher than that in non-pulmonary metastatic osteosarcoma ($P < 0.01$). The level of MVD in pulmonary metastatic osteosarcoma was higher than that in non-pulmonary metastatic osteosarcoma ($P < 0.01$).

Conclusion The expression level of CXCR4 was significantly associated with pulmonary metastasis and angiogenesis of osteosarcoma.

Keywords: osteosarcoma; stromal cell-derived factor-1 (CXCL12); chemokine receptors-4 (CXCR4) angiogenesis; pulmonary metastatics

Received: 5 December 2016

Revised: 15 June 2017

Accepted: 18 November 2017

Metastasis is a complex, non-randomized, and multi-step process that involves critical steps such as tumor cell motility, adhesion, invasion, growth, angiogenesis, metastasis-specific organ homing [1], and escape from the immune system [2]. In recent years, many studies have indicated that the biological axis constituted by

stromal cell-derived factor-1 (CXCL12) and chemokine receptors-4 (CXCR4) plays an important role in a variety of tumor and organ-specific metastases [3–6]. In this study, we analyzed CXCL12/CXCR4 expression levels in osteosarcoma and their relationship with angiogenesis.

Materials and Methods

Clinical data

Osteosarcoma primary tumor specimens from 40 patients (22 males, 18 females) were collected. Patients ranged in age from 7 to 45 years, with a mean age of 25.5 years. All samples were collected after obtaining informed consent, with complete clinical data. No patients underwent radiotherapy or chemotherapy before surgery. All cases were confirmed by histology. Among these cases, 16 had lung metastasis and 24 were non-metastatic. Nineteen cases occurred in the femur, 12 in the tibia and fibula, and 9 in the humerus. Histological classification of bone tumors was determined based on WHO classification [7]: 20 cases were in osteoblasts, 10 in cartilage cells, 8 in fibroblasts, and 2 were small cell type.

Immunohistochemistry SP detection

Mouse anti-human CXCL12 monoclonal antibody, mouse anti-human CXCR4 monoclonal antibody, and mouse anti-human CD34 monoclonal antibody were obtained from DAKO Cytomation (Glostrup, Denmark). The S-P kit was purchased from Fuzhou Maixin Company (Fujian, China). Breast cancer specimens were used as positive controls and phosphate-buffered saline as a negative control for the primary antibodies. Immunohistochemical SP staining was conducted according to the kit instructions. Immunohistochemical staining slides were evaluated by two pathologists. Ten fields were counted on each slide at 400× magnification. The percentage of positive cells was determined. Less than 10% were negative, 11%–25% were weakly positive, 25%–50% were middle positive, and 50% were strongly positive. Based on the intensity of staining, no color was considered negative, light brown yellow as weak positive, brown yellow as middle positive, and brown as strong positive. The number of microvascular vessels for 5 fields was counted at 400× magnification and considered the microvessel density (MVD) of each sample.

Real-time fluorescence quantitative PCR

We used the 7500 real-time fluorescence quantitative PCR instrument (Applied Biosystems, Foster City, CA, USA) for SYBR real-time fluorescent quantitative PCR detection to analyze CXCL12 and CXCR4 expression in osteosarcoma; human β -actin [220 base pairs (bp)] was used as an internal reference. The PCR primer sequences and lengths of the amplified fragment were as follows: CXCL12 forward: 5'-CCGCGCTCTGCCTCAGCGACGGGAAG-3', CXCL12 reverse: 5'-CTTGTTTAAAGCTTTCTCCAGGTACT-3' (227 bp); CXCR4 forward: 5'-AGCTGTTGGTAAAAGTGGTCTATG-3', CXCR4 reverse: 5'-GCCTTCTGGTGGCCCTTGAGTGTG-3' (260 bp); β -actin

forward: 5'-CCCAAGGCCAACCGCGAGAAGAT-3', β -actin reverse: 5'-GTCCCGGCCAGCCAGGTCCAG-3' (220 bp).

The reaction conditions for PCR were as follows: 1 cycle at 95 °C for 10 s, 40 cycles at 95 °C for 1 s, 40 cycles at 56 °C for 5 s, and 40 cycles at 72 °C for 35 s. After the reaction, the critical point set in the PCR amplification was determined. The initial fluorescence signal compared to that of the index growth phase at the inflection point corresponding to the number of cycles (threshold cycle, CT) was used as an indirect indicator of the initial concentration of template. The different concentrations of standard template versus the corresponding CT values were plotted to obtain a standard curve.

Statistical analysis

We used SPSS version 10.0 software (SPSS, Inc., Chicago, IL, USA) to analyze the experimental data. A critical value of $P < 0.05$ was considered to indicate a statistically significant difference.

Results

Expression of CXCL12 and CXCR4

CXCL12 protein was mainly located in the cell membrane and/or cytoplasm and showed brown granular staining (Fig. 1). CXCR4 was strongly expressed in osteosarcoma of lung metastasis (Fig. 2) and weakly expressed in osteosarcoma of non-lung metastasis (Fig. 3). The positive rates of CXCL12 and CXCR4 protein expression in osteosarcoma were 40.0% (16/40) and 60.0% (24/40), respectively.

After real-time fluorescence quantitative PCR to detect CXCL12 and CXCR4 expression, we compared CXCL12 and CXCR4 mRNA copy numbers to that of β -actin. Melting curve analysis showed that the CXCR4 PCR melting curve peak was at 86.5 °C. The solution temperature was uniform and the peak was sharp (Fig. 4). The CXCL12 PCR melting curve peak was at 83.5 °C. The solution temperature was uniform and the peak shape was sharp (Fig. 5). All data agreed with the immunohistochemical SP staining results.

Relationship between CXCR4 expression and osteosarcoma lung metastases

In 24 cases of osteosarcoma without pulmonary metastasis, the positive expression of CXCR4 was 41.7%. In 16 patients with lung metastasis of osteosarcoma, CXCR4 expression was 87.5%. CXCR4 expression was significantly different between patients with and without lung distant metastasis ($P = 0.01$) (Table 1). There was no significant correlation with age, tumor size, sex, tumor location, and histological type (Table 2).

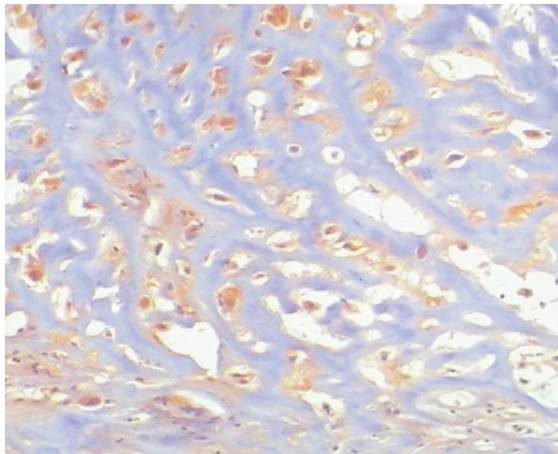


Fig. 1 CXCL12 positive osteosarcoma (×100)

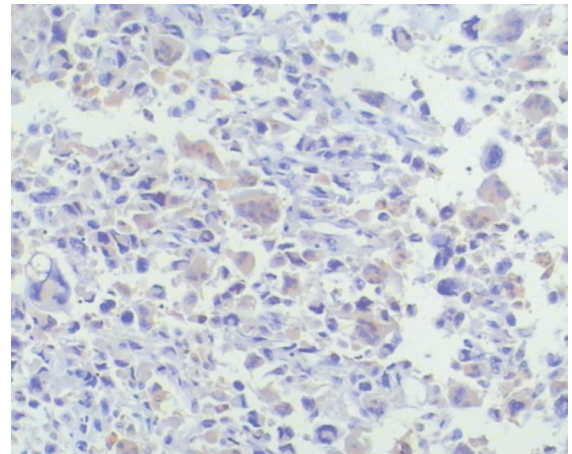


Fig. 2 CXCR4 strongly positive osteosarcoma (×100)

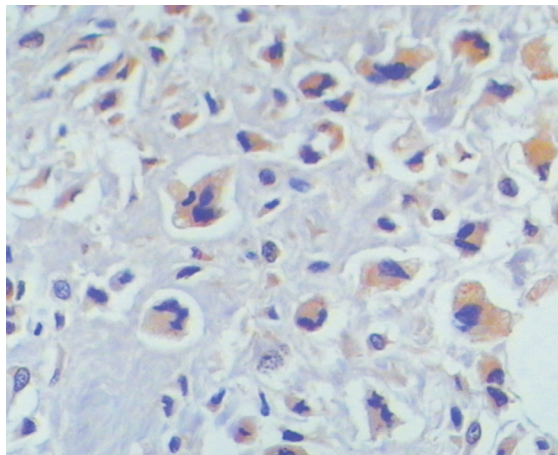


Fig. 3 CXCR4 weakly positive osteosarcoma (×100)

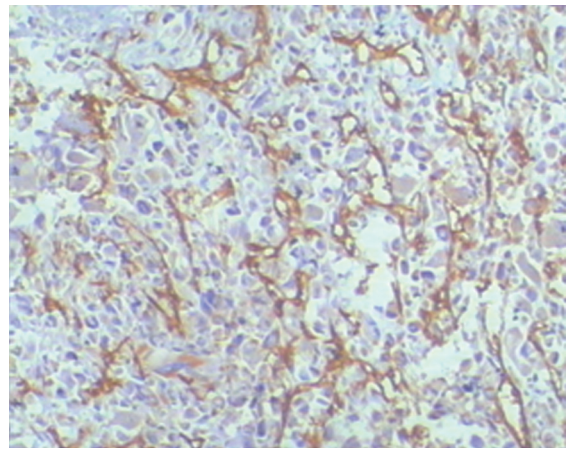


Fig. 6 CD34 positive microvascular endothelial cells (×100)

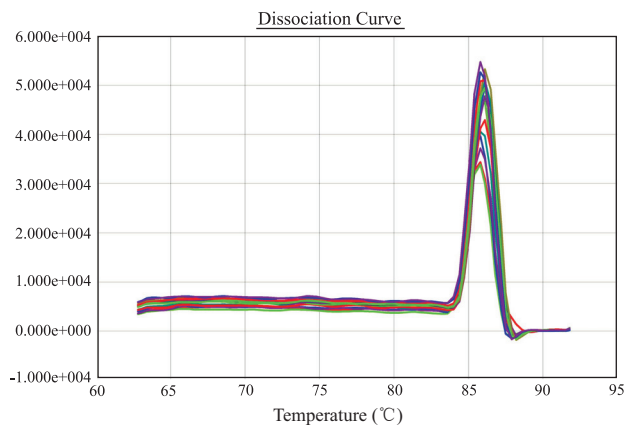


Fig. 4 CXCR4 melting curve

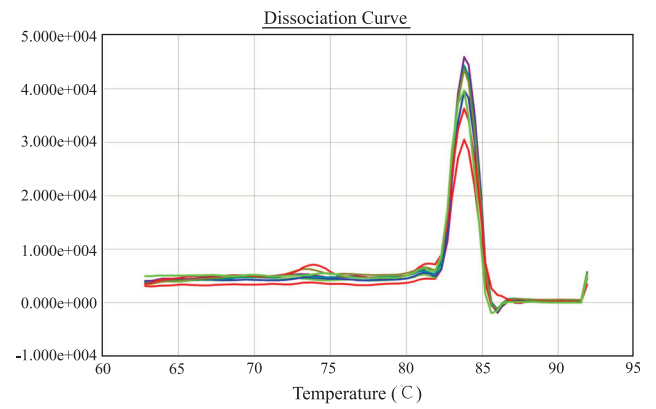


Fig. 5 CXCL12 melting curve

Table 1 Expression of CXCR4 in osteosarcoma (n)

Groups	n	CXCR4 (P < 0.05)	
		Negative	Positive (%)
No metastasis of osteosarcoma	24	14	10 (41.7)
Metastasis of osteosarcoma	16	2	14 (87.5)

Table 3 Relationship between MVD and pulmonary metastasis of osteosarcoma

Groups	n	MVD (P < 0.01)
No metastasis of osteosarcoma	24	64 ± 6.9
Osteosarcoma pulmonary metastasis	16	55 ± 7.0

Relationship between MVD expression and osteosarcoma lung metastases

CD34 was mainly localized in microvascular endothelial cells, according to immunohistochemical staining (Fig. 6). The shape of microvessels in osteosarcoma tissues was irregular and the distribution was uneven. The vascular around the tumor edge was dense, tufted, and sprouting. The microvessels were unevenly distributed. We found that MVD of patients with osteosarcoma lung metastasis was significantly higher than that in patients without metastasis (P < 0.01) (Table 3).

Discussion

Osteosarcoma is the most common malignant bone tumor in children and adolescents [8]. It may show local invasive growth or metastasis. The lung is the most common metastatic site for osteosarcoma [9]. Despite the use of chemotherapy and surgery, 40%–50% of patients experience lung metastases and the 5-year survival rate is only approximately 28% [10].

Muller *et al* [11] first reported human breast cancer cell lines with high expression of chemokine receptor CXCR4 and CCR7 in 2001. Primary breast cancer cells also highly express CXCR4 and CCR7. In breast cancer metastasis sites such as the lymph nodes, lung, liver, and bone marrow, the ligands CXCL12 and CCL21 (6Ckine) are highly expressed. Proteins not from skin and muscle but from lung and liver tissue show significant chemotaxis to breast cancer cells. Muller *et al* verified the hypothesis that tumor cells use chemokines and determined the relationship between cancer and chemokines. To clarify the mechanism of tumor metastasis to search new drugs with anti-metastatic mechanisms, Abu-Khalaf *et al* [12] conducted breast cancer microarray analysis of CXCR4 protein expression and cellular localization in tumor cells. They found that CXCR4 expression in the membrane and cytoplasm was associated with a low survival rate of patients. Another study [13] found that CXCR4 is highly expressed in gastric lymph nodes and

Table 2 Relationship between CXCR4 expression and clinical pathological factors of osteosarcoma (n)

Clinical pathological factors	n	CXCR4 expression		
		Negative	Positive	P
Gender				0.798
Male	22	10	12	
Female	18	8	10	
Age (year)				0.948
≤ 18	19	8	11	
> 18	21	8	13	
Tumor diameter (CM)				0.845
≤ 10	17	7	10	
> 10	23	9	14	
Tumor location				0.898
Femur	19	8	11	
Tibia and fibula	12	5	7	
Humerus	9	3	6	
Organization credit (WHO)				1.000
Osteoblast type	20	8	12	
Cartilage cell type	10	4	6	
Small cell type	2	1	1	
Fibroblast type	8	3	5	

lymphatic vessels. CXCR4 can induce chemotaxis and invasion of tumor cells. CXCR4+ cancer cell lines exhibit significant dose-dependent chemotaxis to CXCL12. High expression of CXCR4 may determine the direction and location of lymph node metastasis. CXCR4 expression detected by endoscopic biopsy may help predict lymph node metastasis and lymph node dissection to determine the surgery range.

In this study, the positive rates of CXCL12 and CXCR4 protein expression in osteosarcoma were 40.0% (16/40) and 60.0% (24/40), respectively. Real-time PCR confirmed these results. CXCR4 protein levels in patients with osteosarcoma lung metastases were significantly higher than those in patients without metastases (P < 0.05).

From the perspective of embryology and histology, generalized angiogenesis can be divided into vasculogenesis and angiogenesis. The former refers to endothelial mesoderm-derived precursor cells (endothelial progenitor cell, EPC) or vascular stem cells (angioblasts; also known as hemangioblastoma or hemangioblasts). Through differentiation and the cluster period, the original vascular network forms during repeated remodeling formation. The angiogenesis process occurs when endothelial cells in pre-existing mature tissue proliferate and migrate by sprouting or intussusceptions in new blood vessels. The concept of angiogenesis had a new breakthrough in 1997. Asahara *et al* [14] detected endothelial precursor cells in adult peripheral blood, indicating that angiogenesis in adults not only occurred during capillary endothelial

cell proliferation and migration, but also contributed angioblasts as vascular endothelial precursors. The formation of new blood vessels involves three steps: angiogenesis, which includes the formation of pre-mature somatic mesoderm tissues in the blood vessel; second, the cell enters the vascular tissue formed from the initial capillary network; third, trimming and transformation into a functional cycle network. Vascular endothelial growth factors such as vascular endothelial growth factor (VEGF) play important roles in the angiogenesis process.

Microvessel counting is commonly conducted to evaluate tumor angiogenesis. Polyclonal anti-CD34 antibody shows high sensitivity for labeling endothelial cells. Our study confirmed that CD34 was localized in microvascular endothelial cells. Microvessels in osteosarcoma exhibit irregular shapes and uneven distributions. The vascular around the tumor edge was dense, tufted, and sprouting as well as unevenly distributed. We found that MVD of patients with osteosarcoma lung metastasis was significantly higher than that of patients without metastasis ($P < 0.01$).

Recent studies^[15] showed that CXCL12 and CXCR4 play important roles in solid tumor growth, metastasis, angiogenesis. Neovascularization is necessary for solid tumor growth. Generally, angiogenesis-promoting chemokines promote tumor formation and inhibiting these chemokines could be anti-tumorigenic. In the VEGF-CXCL12/CXCR4 chain, CXCL12 increases the expression of VEGF and VEGF increases CXCL12 expression. This forms an amplification circuit that is significantly affected by hypoxia. Salvucci *et al*^[16] found that VEGF promotes the expression of CXCL12 in endothelial cells, as well as blocks CXCL12/CXCR4 function and has an anti-angiogenic effect. Koshiha *et al*^[17] found that CXCL12 and the ligands of CXCR4 can promote the formation of blood vessels in the tumor and the migration of tumor cells, leading to rapid tumor growth. We found that MVD expression in the CXCL12-negative group was significantly higher than that in the positive group. This indicates that CXCL12 protein expression and MVD are significantly negatively correlated, which is inconsistent with the results of Salvucci. Cui *et al*^[18] found that CXCR4-CXCL12 induced angiogenesis and lymph node metastases of pancreatic cancer and that adjacent tissues and pancreatic lymph nodes expressed moderate levels of CXCL12 protein. We hypothesize that the VEGF-CXCL12/CXCR4 adjusted chain is related not only to the tumor tissue but also the microenvironment.

Our study confirmed that CXCL12/CXCR4 may play important roles in the progression of osteosarcoma. These results should be confirmed in an animal model of osteosarcoma and *in vivo* and *in vitro* experiments are needed to further verify the CXCL12/CXCR4 mechanism in osteosarcoma.

Institutional review board statement

This case report was reviewed and approved by the Shandong Cancer Hospital & Institute Institutional Review Board.

Informed consent statement

The patients involved in this study gave written informed consent authorizing the use and disclosure of protected health information.

Conflict of interest

The authors indicated no potential conflicts of interest.

References

- Mühlethaler-Mottet A, Liberman J, Ascensão K, *et al*. The CXCR4/CXCR7/CXCL12 axis is involved in a secondary but complex control of neuroblastoma metastatic cell homing. *PLoS One*, 2015, 10: e0125616.
- Lussier DM, Johnson JL, Hingorani P, *et al*. Combination immunotherapy with α -CTLA-4 and α -PD-L1 antibody blockade prevents immune escape and leads to complete control of metastatic osteosarcoma. *J Immunother Cancer*, 2015, 3: 21.
- Xu QH, Wang Z, Chen X, *et al*. Stromal-derived factor-1 α /CXCL12-CXCR4 chemotactic pathway promotes perineural invasion in pancreatic cancer. *Oncotarget*, 2015, 6: 4717–4732.
- Zhao SQ, Wang J, Qin CY. Blockade of CXCL12/CXCR4 signaling inhibits intrahepatic cholangiocarcinoma progression and metastasis via inactivation of canonical Wnt pathway. *J Exp Clin Cancer Res*, 2014, 33: 103.
- Sun YN, Mao XY, Fan CF, *et al*. CXCL12-CXCR4 axis promotes the natural selection of breast cancer cell metastasis. *Tumour Biol*, 2014, 35: 7765–7773.
- Liao YX, Zhou CH, Zeng H, *et al*. The role of the CXCL12-CXCR4/CXCR7 axis in the progression and metastasis of bone sarcomas (Review). *Int J Mol Med*, 2013, 32: 1239–1246.
- Schajowicz F, Sissons HA, Sobin LH. The World Health Organization's histologic classification of bone tumors. A commentary on the second edition. *Cancer*, 1995, 75: 1208–1214.
- Ottaviani G, Jaffe N. The epidemiology of osteosarcoma. *Cancer Treat Res*, 2009, 152: 3–13.
- Huang G, Nishimoto K, Yang Y, *et al*. Participation of the Fas/FasL signaling pathway and the lung microenvironment in the development of osteosarcoma lung metastases. *Adv Exp Med Biol*, 2014, 804: 203–217.
- Kempf-Bielack B, Bielack SS, Jürgens H, *et al*. Osteosarcoma relapse after combined modality therapy: an analysis of unselected patients in the Cooperative Osteosarcoma Study Group (COSS). *J Clin Oncol*, 2005, 23: 559–568.
- Müller A, Homey B, Soto H, *et al*. Involvement of chemokine receptors in breast cancer metastasis. *Nature*, 2001, 410: 50–56.
- Abu-Khalaf MM, Wheler J, Zerkowski M, *et al*. High expression of the chemokine receptor CXCR4 is associated with worse outcome in breast cancer. *ASCO Meeting Abstracts*, 2005, 23: 9593.
- Schimanski CC, Bahre R, Gockel I, *et al*. Chemokine receptor CCR7 enhances intrahepatic and lymphatic dissemination of human hepatocellular cancer. *Oncol Rep*, 2006, 16: 109–113.
- Asahara T, Murohara T, Sullivan A, *et al*. Isolation of putative

- progenitor endothelial cells for angiogenesis. *Science*, 1997, 275: 964–967.
15. Patrussi L, Baldari CT. The CXCL12/CXCR4 axis as a therapeutic target in cancer and HIV-1 infection. *Curr Med Chem*, 2011, 18: 497–512.
 16. Salvucci O, Yao L, Villalba S, *et al*. Regulation of endothelial cell branching morphogenesis by endogenous chemokine stromal-derived factor-1. *Blood*, 2002, 99: 2703–2711.
 17. Koshiba T, Hosotani R, Miyamoto Y, *et al*. Expression of stromal cell-derived factor 1 and CXCR4 ligand receptor system in pancreatic cancer: a possible role for tumor progression. *Clin Cancer Res*, 2000, 6: 3530–3535.
 18. Cui K, Zhao WH, Wang C, *et al*. The CXCR4-CXCL12 pathway facilitates the progression of pancreatic cancer via induction of angiogenesis and lymphangiogenesis. *J Surg Res*, 2011, 171: 143–150.

DOI 10.1007/s10330-016-0211-1

Cite this article as: Han L, Shen YY, Zhao WH, *et al*. Expression of CXCL12-CXCR4 in osteosarcoma and its correlation with angiogenesis *Oncol Transl Med*, 2017, 3: 254–259.

A comparative study between flattening filter-free beams and flattening filter beams in radiotherapy treatment

Ali Wagdy¹, Khaled El Shahat², Huda Ashry³, Amaal El Shershaby⁴, Ehab Abdo²

¹ Al Galaa Oncology Center, Egypt

² Clinical Oncology Department-Faculty of Medicine-Al Azhar University, Cairo, Egypt

³ National Center for Radiation Research and Technology-AEA, Egypt

⁴ Physics Department Women College for Arts Science and Education-Ain Sham University, Cairo, Egypt

Abstract

Flattening filter-free (FFF) beams generated by medical linear particle accelerators (linacs) have recently been used in radiotherapy clinical practice. FFF beams have fundamental physical parameter differences with respect to standard flattening filter (FF) beams, such that the generally used dosimetric parameters and definitions are not always viable. This study investigates dosimetric parameters for use in the quality assurance of FFF beams generated by medical linacs in radiotherapy. The main characteristics of the photon beams are analyzed using specific data generated by a Varian TrueBeam linac having both FFF and FF beams of 6 and 10 MV (megavolt) energy, respectively. Definitions for dose profile parameters are suggested, starting from the renormalization of the FFF with respect to the corresponding FF beam. From this point, the flatness concept is translated into one of “un-flatness”, and other definitions are proposed, maintaining a strict parallelism between FFF and FF parameter concepts. The quality controls used in establishing a quality assurance program when introducing FFF beams into the clinical environment are given, maintaining similarity to those used for standard FF beams, and recommendations for the introduction of FFF beams into clinical radiotherapy application for breast cancer patients are provided as an example for comparison between FFF and FF for dose distribution and coverage for a target volume. Although there are many advantages of using a FFF beam, especially for advanced radiotherapy techniques, there are a few limitations (e.g., using a relatively higher energy photon beam for stereotactic radiotherapy (SRT), limited speed of current multileaf collimators (MLCs), and off-axis distance-dependent modulation in intensity-modulated radiation therapy (IMRT)) as well as challenges (e.g., criteria for beam quality evaluation and penumbra, establishment of dosimetry methods, and consequences of photon target burn-up) that need to be addressed for establishing the FFF beam as a viable alternative to the FF beam.

Keywords: flattening filter-free beam; flattening filter beam; breast cancer; treatment planning; beam characteristics; multileaf collimator

Received: 8 August 2016

Revised: 11 October 2016

Accepted: 23 May 2017

Traditionally, the flattening filter (FF) in the X-ray beam path of a linear accelerator produces an almost uniform fluence over a collimated field. This is particularly advantageous for 3D conformal radiation therapy (CRT) for practical reasons.

The removal of the FF leads to a rapidly decreasing fluence distribution, and thus to inhomogeneous dose distributions. The advantage of this is its positive

influence on the peripheral dose through reduced head scatter and MLC leakage ^[1], as well as a considerable increase in the dose rate, which has a beneficial effect on modern therapy methods.

In addition to improved shielding in the treatment head, Ponisch *et al* ^[2] suggest the use of secondary jaws to track the MLC and removal of the FF as a source of scattered radiation with fluence-modulated radiation therapy

✉ Corresponding to: Khaled El Shahat. Email: khelshahat@yahoo.com

(RT). The disadvantage of a non-uniform, conical fluence distribution can be considered with intensity-modulated radiation therapy (IMRT) in an optimization algorithm. Recent studies show the feasibility of using flattening filter-free (FFF) beams for IMRT and stereotactic body radiation therapy (SBRT) [3–5]. In addition, it has been concluded that the decreased variation in scatter factors and beam quality along the field simplifies the dose calculation [6]. It is often necessary to resort to field-in-field (FIF) techniques, also referred to as forward IMRT techniques, to achieve better conformity for the PTV in 3D CRT planning. Additional fields in one angle of incidence (multistatic field) can be used to adapt dose distribution optimally to the anatomy of the patient without the need for a wedge. Several studies for various RT locations show that a beneficial dose distribution can be achieved with this method with regard to homogeneity and conformity [7–9]. It is also possible to use FFF beams in 3D CRT through this FIF technique.

Materials and methods

Materials

Linear accelerator—TrueBeam system

The linear accelerator used in this study is a TrueBeam linac developed by Varian Medical Systems. It is designed to deliver FF as well as FFF photon beams. It represents a new platform of Varian linacs, where many key elements, including the waveguide system, carousel assembly, beam generation, and monitoring control system, differ from the preceding CLINAC series. Further, it contains a multiport X-ray filter management system (carousel) that accommodates field-flattening filters and open ports. The dosimetry systems of these linacs (monitor chamber) are capable of accurately processing a wide range of ionizations per pulse. The maximum dose rates of the TrueBeam system are 1400 and 2400 MU/min for 6 MV (labeled as 6XFFF) and 10 MV (labeled as 10XFFF) X-rays, respectively. The accelerator is equipped with asymmetric collimation jaws and an MLC consisting of 120 leaves on each side, allowing a maximum field size of $40 \times 40 \text{ cm}^2$.

Dosimetry system

A PTW MP3 water phantom (PTW Freiburg GmbH) with inner tank dimensions of $694.0 \times 596.0 \times 502.5 \text{ mm}^3$ is used together with a cylindrical semiflex ion-chamber (PTW, type 21010) with an inner cavity volume of 0.125 cm^3 . Further, to compensate for beam output variations, a cylindrical ion-chamber (PTW, type 31010) was used as a reference in the present and all the following relative dose measurements.

PTW UNIDOS electrometer

For all measurements with the water tank scanning system, a PTW UNIDOS Electrometer is used, and the

data collection is performed using the PTW MEPHYSTO software.

Vascular slices showed sharply cut edges with blood vessels. Outside the cut edge, the vessel wall and surrounding tissue were thick, and had long endovascular thrombosed segments.

Portal Dosimetry

During this work, Electronic Portal Imaging Devices (EPID) are used for acquiring megavoltage images during patient treatment. The larger area of the Digital Megavolt Imagers (DMI) is a square ($43 \times 43 \text{ cm}^2$ for single images).

Methods

Linear accelerator—TrueBeam system

For each photon energy, percentage depth dose curves (PDDs) are acquired for 13 square field sizes: 2, 3, 4, 6, 8, 10, 12, 15, 20, 25, 30, 35, and 40 cm. Field size is defined by jaws, not MLC, due to the standard data collection measured for jaws only, and after all data commissioning, then scatter from MLCs measured and add for data transfer for treatment planning system for creation different shapes for field sizes.

The water level is checked periodically using the front pointer – always before the first scan – for X6 and 6FFF additionally at mid-field size. Evaporation makes it necessary to fill the water tank approximately every 30 minutes, depending on room temperature and humidity. The front pointer method can detect changes of SSD in the order of 0.2 mm.

On one hand, the depths for maximum dose (d_{max}) serve as reference depths for the linac output calibration. Following the Varian recommendation, we calibrate our TrueBeams to deliver 1.0 Gy per 100 MU at an SSD of 100 cm at a depth of d_{max} for the $10 \times 10 \text{ cm}^2$ reference field.

Results

D_{max} results

The following d_{max} depths for the $10 \times 10 \text{ cm}^2$ field were determined:

- 16 mm (X6)
- 14 mm (6FFF)
- 26 mm (X10)
- 24 mm (10FFF)

Figs. 1 and 2 show the PDDs for all field sizes (from 2.0 cm^2 to 40 cm^2) for 6 MV (FF and FFF). Figs. 3 and 4 show the beam profiles for all field sizes (from 2.0 cm^2 to 40 cm^2) for 6 MV (FF and FFF).

Figs. 3 and 4 show the beam profiles for field size $40 \times 40 \text{ cm}^2$ for 6 MV (FF and FFF), from which the following observations can be made:

Sm: in the plateau region, all profiles were smoothed once.

For the two FFF energies only, a single data point was

added to the 40×40 cm² profile at 300 mm depth, at the location -294.5 mm. The data point value was guessed visually.

Sym: all profiles were mirrored (symmetries).

The saturation correction of transverse profiles is shown in analogy to the PDD curves. However, we find that it does not make sense to correct the profiles for saturation. While for a PDD at the lowest energy (6FFF), the dose per pulse ratio between d_{\max} and 300 mm depth can be up to 6.7 (the PDD value of 6FFF, field size 1×1 cm, at 300 mm depth, is 14.9%), the dose per pulse at the shoulder point of a FFF cross-plane profile is at least 40% (10FFF, 40×40 cm², 22 mm depth). As the transverse profiles are always normalized to the central axis (CAX) during TPS formatting, a saturation correction of the profiles would have no effect between the CAX and the shoulder point, from which it can be concluded that the effect is smaller than 0.1%.

The magnitude of contaminating electrons from the FFF beam is relatively small and, therefore, the depth of the dose maximum shows a weak dependence on field-size variation. Lateral dose profiles of the FFF beam differ significantly from those of the FF beam. The central peak in the lateral profiles of the FFF beam is pronounced only for medium to large field sizes. The higher the energy, the more pronounced the central peak is. The shape of the lateral beam profile of a FFF beam changes slightly with depth due to a significantly reduced off-axis softening effect, and hence the depth-dose characteristic remains almost constant across the field, even for large field sizes.

Optimization of dose distribution

The larger area of the Digital Megavolt Imager (DMI) is square (43×43 cm² for single images). This offers the possibility to image larger field lengths at the same imaging distance.

Resolution is also slightly improved. The image size is 1280×1280 pixels for single images.

Case study – 6 MV (FFF)

For the second FFF energy, 6FFF, portal dosimetry results also improved dramatically. Outside the Complete Irradiation Area Outline (CIAO), profiles measured with a Varian aS1000 imager were often very low compared to calculations using EPIQA (EPIQA is non-transit commercial software that can convert a dosimetric image acquired by an EPID into a dose map, and compares the dose map with a reference dose distribution). This problem does not currently exist.

Fig. 5 shows an example of IMRT plan 5 fields of the breast, 6FFF, 1400 MU/min, again measured at isocenter distance. With the 2%/2 mm criterion, the gamma agreement index for both arcs is approximately 100%

over the whole detector area.

As shown in Fig. 5, there is a significant difference between dose distribution for 6 MV (FFF) in target coverage and doses for organs at risk versus 6 MV (FF), due to the difference in depth of the maximum dose and applicability for good distribution with the FFF beam.

The photo-neutron fluence per monitor unit (MU) produced by the high-energy FFF beam is relatively less in comparison to that produced by the FF beam (Fig. 8). Hence, operating the accelerator in the FFF mode benefits both the patient and the radiation therapy technologist. However, the benefit of decreased neutron dose for FFF beams at high X-ray energies (15, 18 MV) needs to be critically examined, giving due consideration to their clinical use over low X-ray energies (6, 10 MV). Due to reduced average energy, treatment head leakage, and fractional neutron dose, the concrete thickness required for the FFF linac vault is also relatively less. Thus, the existing linac vault can safely be used for operating the FFF linac at reduced occupational exposure, and while

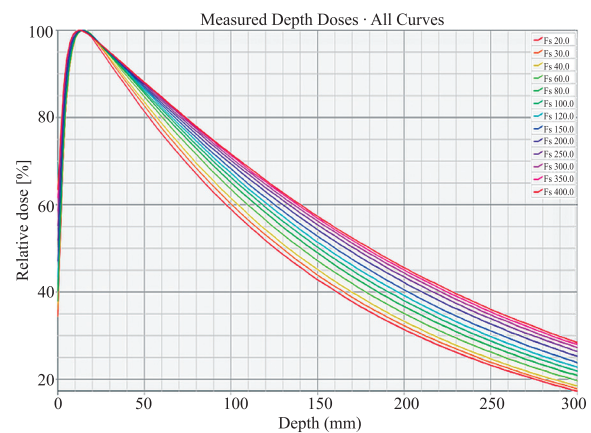


Fig. 1 Percentage depths dose for all field sizes (from 2.0 cm² to 40 cm²) for 6 MV (FF)

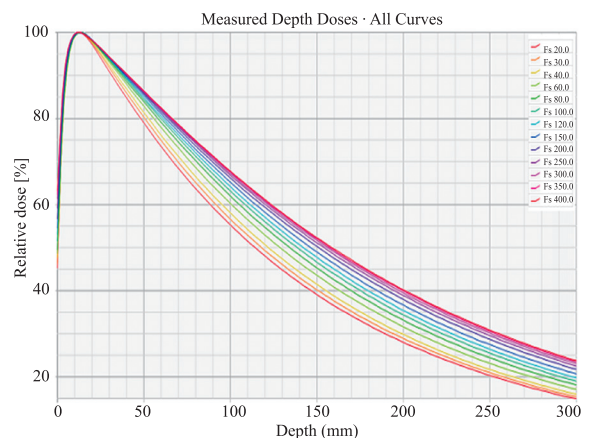


Fig. 2 Percentage depths dose for all field size (from 2.0 cm² to 40 cm²) for 6 MV (FFF)

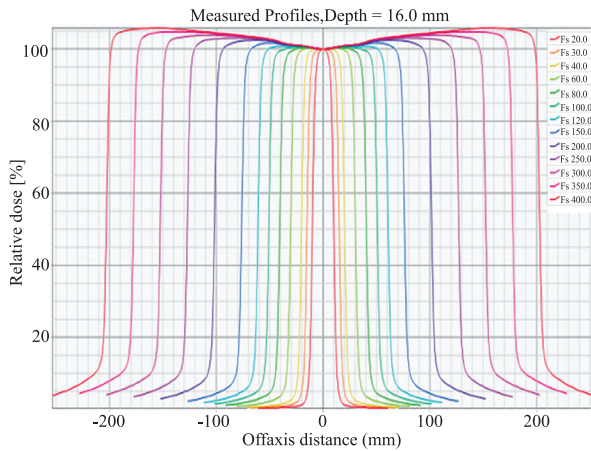


Fig. 3 Beam profiles for all field sizes (from 2.0 cm² to 40 cm²) for 6 MV (FF)

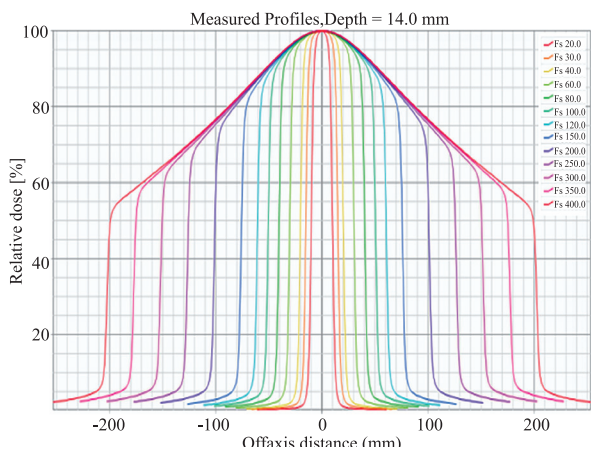


Fig. 4 Beam profiles for all field sizes (from 2.0 cm² to 40 cm²) for 6 MV (FFF)

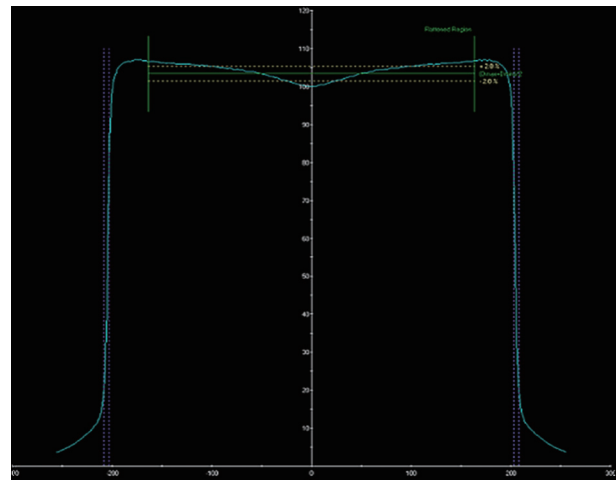


Fig. 5 Beam profile for field size 40 × 40 cm² for 6 MV (FF)

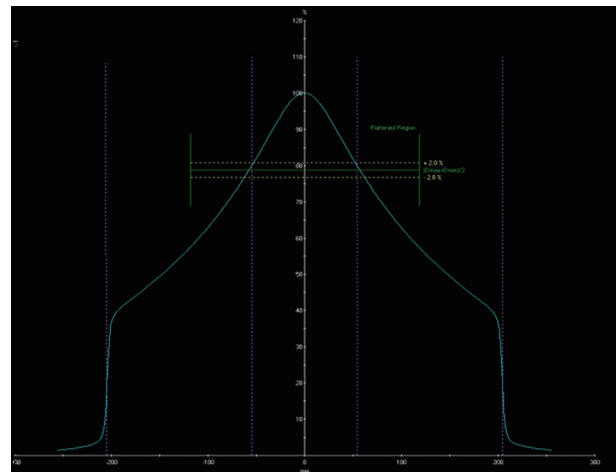


Fig. 6 Beam profile for field size 40 × 40 cm² for 6 MV (FFF)

constructing a new shielded vault there will be a saving of space and cost.

In addition, the phosphor screen of the EPID shows increased sensitivity to low-energy photons present in the spectra of the FFF beam. It was also reported that the EPID-measured profile changes minimally with increasing phantom thickness due to small energy variation across the profile. Portal dosimetry using existing EPID of standard linac is therefore a possible option for patient-specific quality assurance in the FFF beam.

Case study – 10 MV (FFF)

The following example shows palliative treatment of single arc, 10FFF energy, 2400 MU/min and 2357.2 MU total, planned with Eclipse 13.6 (AAA 13.6.23). This plan was verified with portal dosimetry for a single fraction in

palliative cases (Fig. 7).

A verification plan was calculated using a portal dose image prediction (PDIP) algorithm. The arc was measured with the DMI imager at isocenter distance and analyzed using the 3%/3 mm DTA gamma criterion:

Volumetric modulated arc therapy (VMAT), or Varian RapidArc® Radiotherapy Technology, is an advanced form of IMRT that delivers a precisely sculpted 3D dose distribution with 360° as the maximum for angle rotation of the gantry in a single or multi-arc treatment. RapidArc uses a dynamic MLC, variable dose rate, and variable gantry speed to generate IMRT-quality dose distributions.

The current dosimetry protocols that are followed for output measurement of photon beams from medical linear accelerators require a beam quality correction factor. This beam quality correction factor is related to the quality index [%DD(10) or TPR1020] of the photon beam. As the

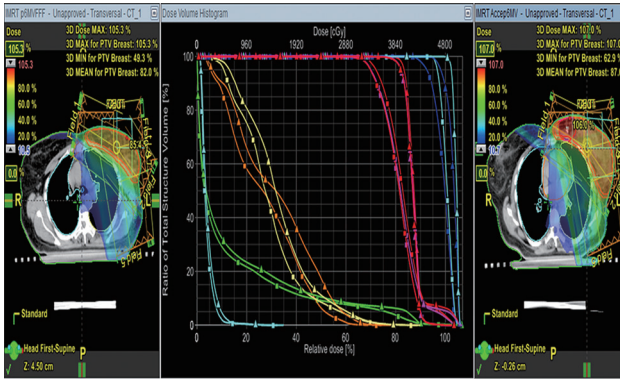


Fig. 7 Comparison for two-dose distribution for breast cancer, plotted at 6 MV (FFF) and 6 MV (FF)

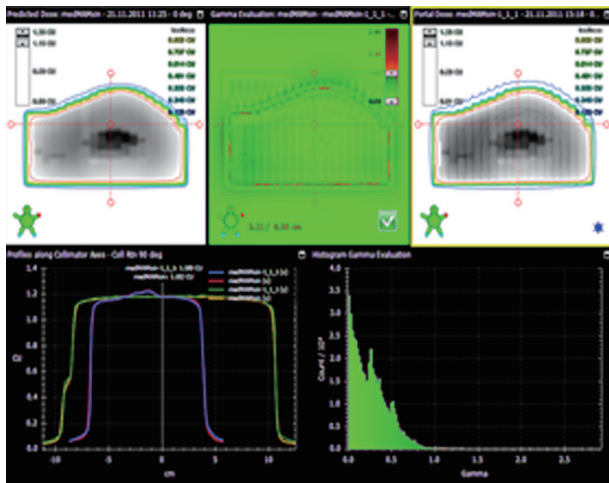


Fig. 8 EPID evaluation of two tangents for a breast cancer patient using FFF, as an example of a portal dosimetry tool for a TrueBeam linear accelerator

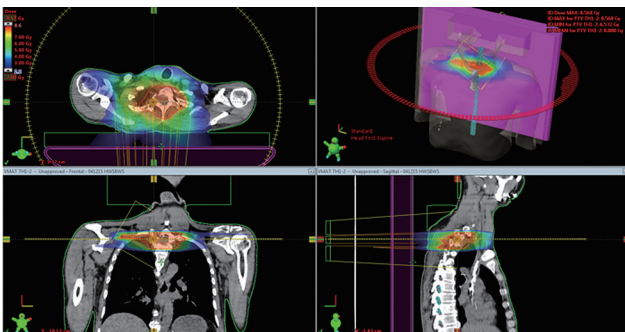


Fig. 9 Example of dorsal lesion for 10 MV FFF beam and dose distribution using the VMAT technique (single arc)

reference conditions for measuring the quality index of the photon beam is given with reference to the FF beam, it cannot be directly applied for the FFF beam. Therefore,

there is a need to revise the existing dosimetry protocols for the FFF beam. The conventional definition of beam penumbra is not applicable to the FFF beam, and requires a modification to the definition. The primary electrons have been reported to penetrate through the high Z thin targets used for generating bremsstrahlung photons, posing a potential risk for producing high surface doses if not removed.

In the case of a standard photon beam (FF), the electrons penetrating through the thin bremsstrahlung targets are efficiently removed by the FF. In a FFF linac, an additional thin metal plate in front of the monitor chamber is used to remove the primary electrons penetrating through the bremsstrahlung target. The material and the thickness of this plate need to be optimized, maintaining the advantage of the FFF beam, and giving due consideration to the incidence of bremsstrahlung target breaks.

Discussion

Advanced beam therapy techniques, such as RT, where inhomogeneous dose distributions are applied, and IMRT, where varying fluence patterns across the beam are delivered, have stimulated interest in operating a standard linac in the FFF mode. A standard linac can be used for generating photon beams with either an FF beam or a FFF beam. Several Monte Carlo and experimental studies dealing with characteristics, dosimetric aspects, and radiation protection issues of FFF photon beams, generated by mechanically removing the flattening filter of existing standard linacs of different makes and models, have been recently reported. Studies related to treatment planning and dose delivery of various clinical cases using FFF beams demonstrate their clinical suitability and superiority over FF photon beams. A review of the properties of FFF photon beams summarizing the findings of different investigators has also been recently published.

A recent study by Hrbacek et al [15] reports the measured dosimetric characteristics of unflattened photon beams generated using a new model of a standard linac (Varian TrueBeam STx), capable of generating both flattened and unflattened clinical photon beams. It is well known that the FF in a standard linear accelerator acts as an attenuator, a beam hardener, and a scatterer. Obviously, the removal of the FF results in an increase in dose rate, softening of the X-ray spectra, and a reduction in head scattered radiation and the non-uniform beam profile. The reported dose rate of FFF beams is about 2–4 times higher than that of the FF beams, that is, FFF linear accelerators can typically be operated at a dose rate higher than 10 Gy/min under the normal operating conditions applied for FF linear accelerators. The increased dose rate decreases the dose delivery time, especially for hypo-fractionated

stereotactic radiotherapy (SRT), and is thought to be useful in managing the intrafractional target motion.

The softening of the X-ray spectra affects the depth as well as the lateral dose distribution at all depths, and results in increased surface dose and slight shifting of the depth of maximum dose toward the surface. The lateral transport is reduced, which may result in greater control over gradients within the field and at target boundaries. The head scatter variation for an unflattened beam is typically about 1.5 % as against about 8 % of the flattened beam for the field sizes in the range from $3 \times 3 \text{ cm}^2$ to $40 \times 40 \text{ cm}^2$.

As a result, a simple model for dose calculation of irregular treatment fields is sufficient for the FFF beam. Moreover, due to the absence of the collimator exchange effect, it is not necessary to account for whether the upper or lower secondary collimator is defining the long side of the rectangular beam. The decreased head scatter, and hence the reduced head leakage, also results in decreased far field peripheral dose (PD) to the patient.

The near field PD is also due less to the combined effects of softer photon beam spectra, increased dose per pulse, and reduced collimator transmission. While treating the patients by radiotherapy (IMRT) with a 6 MV FFF beam, the integral dose to nearby healthy tissue and the whole-body integral dose, respectively, were found to be significantly higher than the FF beam, and the use of higher FFF beam energy is suggested as the remedy for the problem (e.g., using 10 MV instead of 6 MV)^[1]. This is because the 10 MV unflattened depth dose characteristics are similar to those for a 6 MV flattened beam. The use of a FFF beam over a FF beam is a natural choice for IMRT treatments. However, the leaf travel time for creating a large number of optimized segments for static IMRT and the leaf speed for the dynamic and rotational IMRT are the limiting factors in the dose delivery efficiency of IMRT.

Hence, for effective and efficient use of the FFF beam, the technology of current MLCs needs to be modified. Further, the intensity of the FFF beam abruptly decreases with the off-axis distance for large open fields ($\geq 10 \times 10 \text{ cm}^2$), which necessitates the off-axis distance-dependent modulation for delivering uniform dose to the tumor. While executing the off-axis distance-dependent modulation by dynamic MLC, larger monitor units are required, which increase the gross head leakage and lessen the advantage of using the FFF beam. This effect is significant in dynamic IMRT of off-axis targets and large volume targets; while dealing with such clinical cases, a modified FFF beam is required^[16].

Conclusions

Although there are a number of advantages of using

a FFF beam, especially for advanced radiotherapy techniques, there are a few limitations (e.g., using a relatively higher energy photon beam for SRT, limited speed of current MLCs, and off-axis distance-dependent modulation in IMRT) as well as challenges (e.g., criteria for beam quality evaluation and penumbra, establishment of dosimetry methods, and consequences of photon target burn-up) that need to be addressed for establishing the FFF beam as a viable alternative to the FF beam.

Conflict of interest

The authors indicated no potential conflicts of interest.

References

- Vassiliev ON, Titt U, Kry SF, *et al.* Monte Carlo study of photon fields from a flattening filter-free clinical accelerator. *Med Phys*, 2006, 33: 820–827.
- Pönisch F, Titt U, Vassiliev ON, *et al.* Properties of un-flattened photon beams shaped by a multileaf collimator. *Med Phys*, 2006, 33: 1738–1746.
- Cashmore J. The characterization of unflattened photon beams from a 6 MV linear accelerator. *Phys Med Biol*, 2008, 53: 1933–1946.
- Parsai EI, Pearson D, Kvale T. Consequences of removing the flattening filter from LINACs in generating high dose rate photon beams for clinical applications: A Monte Carlo study verified by measurement. *NuclInstrum. Methods Phys Res B* 2007;261:755.
- Kragl G, af Wetterstedt S, Knäusl B, *et al.* Dosimetric characteristics of 6 and 10MV unflattened photon beams. *Radiother Oncol*, 2009, 93: 141–146.
- Dalaryd M, Kragl G, Ceberg C, *et al.* A Monte Carlo study of a flattening filter-free linear accelerator verified with measurements. *Phys Med Biol*, 2010, 55: 7333–7344.
- Titt U, Vassiliev ON, Pönisch F, *et al.* Monte Carlo study of backscatter in a flattening filter free clinical accelerator. *Med Phys*, 2006, 33: 3270–3273.
- Georg D, Kragl G, Wetterstedt S, *et al.* Photon beam quality variations of a flattening filter free linear accelerator. *Med Phys*, 2010, 37: 49–53.
- Kry SF, Howell RM, Titt U, *et al.* Energy spectra, sources, and shielding considerations for neutrons generated by a flattening filter-free Clinac. *Med Phys*, 2008, 35: 1906–1911.
- Sawkey DL, Faddegon BA. Determination of electron energy, spectral width, and beam divergence at the exit window for clinical megavoltage x-ray beams. *Med Phys*, 2009, 36: 698–707.
- Kry SF, Titt U, Pönisch F, *et al.* Reduced neutron production through use of a flattening-filter-free accelerator. *Int J Radiat Oncol Biol Phys*, 2007, 68: 1260–1264.
- Kry SF, Howell RM, Polf J, *et al.* Treatment vault shielding for a flattening filter-free medical linear accelerator. *Phys Med Biol*, 2009, 54: 1265–1273.
- Vassiliev ON, Titt U, Kry SF, Mohan R, Gillin MT. Radiation safety survey on a flattening filter-free medical accelerator. *Radiat Prot Dosimetry*, 2007, 124: 187–190.
- Tsechanski A, Krutman Y, Faermann S. On the existence of low-energy photons (<150 keV) in the unflattened x-ray beam from an ordinary radiotherapeutic target in a medical linear accelerator. *Phys Med Biol*, 2005, 50: 5629–5639.
- Hrbacek J1, Lang S, Klöck S. Commissioning of photon beams of

a flattening filter-free linear accelerator and the accuracy of beam modeling using an anisotropic analytical algorithm. *Int J Radiat Oncol Biol Phys*, 2011, 80: 1228–1237.

16. Tyner E, McClean B, McCavana P, *et al.* Experimental investigation of the response of an a-Si EPID to an unflattened photon beam from an Elekta Precise linear accelerator. *Med Phys*, 2009, 36: 1318–1329.

DOI 10.1007/s10330-016-0183-3

Cite this article as: Ali Wagdy, El Shahat, Khaled M, *et al.* A comparative study between flattening filter-free beams and flattening filter beams in radiotherapy treatment. *Oncol Transl Med*, 2017, 3: 260–266.

Primary urachal adenocarcinoma: a rare case report

Kaihua Liu¹, Hongqiang Wang², Lei Yu², Peitao Wang², Zhijun Liu³, Lijiang Sun⁴, Hongsheng Yu⁵, Shenqian Li² (✉)

¹The Medical College of Qingdao University, Qingdao 266071, China

²Department of Andrology, The Affiliated Hospital of Qingdao University, Qingdao 266003, China

³Department of Clinical Laboratory, The Affiliated Hospital of Qingdao University, Qingdao 266003, China

⁴Department of Urology, The Affiliated Hospital of Qingdao University, Qingdao 266003, China

⁵Department of Oncology, The Affiliated Hospital of Qingdao University, Qingdao 266003, China

Abstract

Primary urachal carcinoma is a very rare cancer with a poor prognosis. It generally presents as a high-grade, high-stage tumor, and in most cases the patient has developed regional or distant metastasis at the time of presentation. Here, we report a very interesting case of primary urachal adenocarcinoma with signet ring cell carcinoma in a 58-year-old male who presented with a lower abdominal mass and discomfort. In this case, urachal carcinoma was successfully treated with surgery using an extended partial bladder cystectomy approach with excision of the urachal mass and umbilicus. The patient also underwent systematic chemotherapy with 5-fluorouracil and cisplatin. During the 12-month follow-up period, the patient did not experience recurrence or metastasis. Overall, we found that an organ preserving extended partial cystectomy along with chemotherapy was an optimal treatment method that helped improve the patient's quality of the life with no recurrence of cancer so far.

Key words urachal tumor; urachus; bladder cancer; therapy

Received: 7 December 2017
Revised: 20 December 2017
Accepted: 28 December 2017

The urachus is a tubular structure that connects the bladder with the umbilicus. Nitrogenous waste is discharged from the bladder, the main organ of excretion during the fetal period. During the fourth and fifth month of embryonic life, the urachus gradually degenerates into a rudimentary fibromuscular closed canal, which is known in adults as the median umbilical ligament, and stretches between the dome of the urinary bladder and the umbilicus. However, a urachal remnant in the form of a tubular or cystic muscular structure can persist. It is most commonly found between the umbilicus and the bladder, usually at the dome of the bladder. After birth, if the umbilical lumen is not completely closed, it may lead to various abnormalities including infection, cystic degeneration, and malignancy [1]. Autopsy studies suggest that in one-third of adults, the urachus canal partly persists [2]. Urachal carcinoma (URC) is a rare malignant disease that manifests in residual urinary tissue, accounts for 0.01% of adult tumors and approximately 20% to 40% of primary bladder adenocarcinomas [3]. Urachal tumors

tend to be associated with a poor prognosis, with 5-year survival rates ranging from 9.0% to 43% [4].

Case report

A 58-year-old male, with no smoking history, presented to us with a lower abdominal lump approximately 5.0 × 3.0 cm in size. The lump had started to develop five years prior and grew gradually each year. As the lump grew, he also felt discomfort. He had no previous history of hematuria, cystitis cystica, cystitis glandularis, bladder irritation or weight loss. However, the patient had a 24-year history of hypertension for which he took medication.

On physical examination, a well-defined lump was palpable in the umbilical and hyponastic region and was globular in shape. It was approximately 12 × 10 cm in size, had smooth surface and regular margins all around. No abnormalities were found in the rest of the physical examination. Ultrasonography showed a solid

and cystic heterogenous, uneven mass approximately $12.4 \times 10.1 \times 9.2$ cm above and close to the left wall of the bladder. The ultrasound also showed evidence of adequate bladder filling, smooth mucosa and no obvious significant mass. The urine microscopy and urine cytology did not reveal any abnormalities. Computed Tomography (CT) of the abdomen showed a hypodense soft tissue lesion in the supravescical region near the dome of the urinary bladder; the lesion extended superiorly up to just below the umbilicus, and therefore the border between the lower margin and the bladder was not clear (Fig. 1). There was no evidence of distant metastasis or intra-abdominal lymphadenopathy and the other organs appeared normal. The provisional diagnosis was a urachal



Fig. 1 Computed Tomography of abdomen showing urachal mass (arrow) attaching the bladder dome and squeezed the bladder

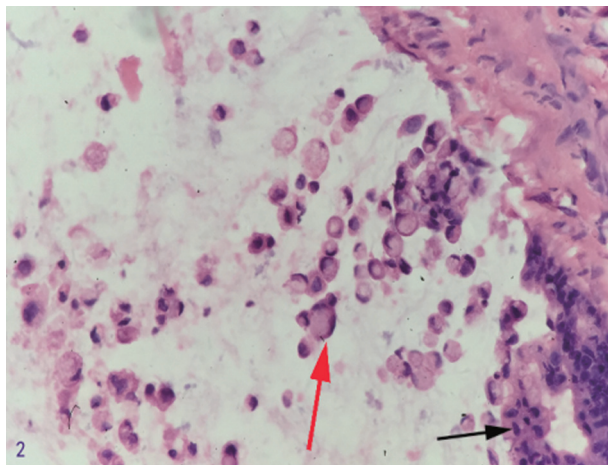


Fig. 2 Histopathological findings of the biopsy showing the tumour cells containing intracellular vacuole displacing the hyperchromatic nucleus to one side suggestive of signet ring cell carcinoma (red arrow), | urachal mucinous adenocarcinoma (black arrow)

remnant malignancy. The patient underwent cystoscopic examination, which revealed a round swollen area of tissue that was squeezing the anterior dome of the bladder; the bladder mucosa was smooth.

Surgical exploration was performed for the patient after adequate preoperative preparation. During the exploration, a urachal mass extending up to the dome of urinary bladder was found. The mass was approximately $12.0 \times 10.0 \times 9.0$ cm in size and was not interlinked with the bladder. Surrounding it was approximately 200 milliliters of a viscous secretion. An extended partial cystectomy with excision of the urachal mass and umbilicus was performed after confirming the absence of leakage from the urinary bladder. After the operation, the patient received 6 cycles of systemic chemotherapy which included 5-fluorouracil (FU) and cisplatin.

Pathological analysis revealed a urachal mucinous adenocarcinoma, with partial signet ring cell carcinoma; there was no evidence of deep invasion through the urachus, and the incisal margin of the bladder was negative (Fig. 2). The Myao stage at diagnosis is I period. The patient has been regularly followed-up for 12 months and doing is well.

Discussion

Primary urachal adenocarcinoma is an extremely rare but highly malignant tumor, accounting for only 0.17 to 0.34 % of all bladder tumors [5]. This tumor is more common in males aged from 40 to 60 years. To date, no consensus has been reached regarding the diagnostic criteria of URC. The most commonly used criteria have been proposed by Sheldon *et al* [6] and Mostofi *et al* [7] and revised by Gopalan *et al* [5] which include the following characteristics: (1) tumor is located in the dome/anterior wall of the bladder, (2) the tumor is located at the epicenter in the bladder wall, (3) there is an absence of cystitis cystica and cystitis glandularis, and (4) lack of known primary adenocarcinoma elsewhere. The most common symptoms of URC include macroscopic or microscopic hematuria, abdominal pain, and dysuria. Other less common clinical presentations included pollakisuria, pyuria, urinary tract infection, umbilical discharge (e.g. blood, urine, and mucus), vaginal discharge, and nonspecific symptoms (nausea, vomiting, diarrhea, weight loss, or fever) [8]. Some serum markers have proven to be helpful in the diagnosis and monitoring of URC, including carcinoembryonic antigen and carbohydrate antigen 19-9 as well as cancer antigen 125. Increased serum levels of these markers have been detected in patients with URC adenocarcinoma [9, 10]. In this case, the patient presented with a mass in the abdomen, no hematuria or abdominal pain, absent typical clinical symptoms such as ___ and the serum markers appeared normal. When a patient presents with non-

specific symptoms like an abdominal mass in our case, then a high index of suspicion is required because these symptoms are very common with benign conditions. The most common pathological type of urachal tumor is adenocarcinoma. Other rare patterns include the signet ring cell type, clear cell type, hepatoid type, and mixed patterns^[11]. It has been postulated that the oncogenesis of urachal adenocarcinoma involves a metaplastic process, as the urachal urothelium often exhibits glandular metaplasia^[5]. Several stage classifications exist, but the most often used is the Mayo staging system^[6], which includes the following: I. Tumor is confined to the urachus and/or bladder, II. Tumor extends beyond the muscular layer of urachus and/or the bladder, III. Tumor infiltrates the regional lymph node, IV. Tumor infiltrates the non-regional lymph nodes or other distant sites. Generally, URC presents as a high-grade, high-stage cancer, and in the majority of cases there is regional or distant metastasis at the time of presentation. Therefore, this cancer is usually associated with a poor prognosis^[12]. By lymphatic dissemination URC usually metastasizes into the pelvic lymph nodes and by hematogenous dissemination into distant organs, especially lungs, bone, or peritoneum^[13]. Although the pathological features of ureteral adenocarcinoma and bladder adenocarcinoma are similar, the prognosis for ureteral adenocarcinoma is better than for bladder adenocarcinoma. This may be due to the age of patients since those with ureteral adenocarcinoma are often younger than those with adenocarcinoma of the bladder^[14]. Surgery remains the primary treatment for prolonging the overall survival of patients. Some scholars believe that both partial and radical cystectomy can be considered as they provide similar oncological results^[15]. However, Behrendt *et al*^[16] suggests that an organ preserving extended partial cystectomy provides a higher quality of life and should be preferred. Since URC is not sensitive to radiotherapy, chemotherapy, along with the surgery, is the only treatment option to potentially prolong survival. One meta-analysis suggested that the most effective treatment may be a combination of 5-FU with cisplatin, which performs significantly better than cisplatin-based only therapies^[8].

URC is an extremely rare cancer and often presents as a high-grade, high-stage cancer. A localized URC organ preserving partial cystectomy provides a long-term disease-free survival, and the combination of 5-FU with cisplatin provides the most favorable response. In addition, regular postoperative follow-up is necessary.

Conflicts of interest

The authors indicated no potential conflicts of interest.

References

1. Irwin PP, Weston PM, Sheridan W, *et al*. Transitional cell carcinoma arising in a urachal cyst. *Br J Urol*, 1991, 67: 103–104.
2. Wilcox DT, Godbole PP, Koyle MA. Pediatric urology: surgical complications and Management, 2009, 181: 2391–2391.
3. Niu HT, Dong P, Wang JN, *et al*. Analysis of treatment and prognosis in post-operative patients with urachal carcinoma. *Natl Med J China (Chinese)*, 2016, 96: 1923–1925.
4. Henly DR, Farrow GM, Zincke H, *et al*. Urachal cancer: role of conservative surgery. *Urology*, 1993, 42: 635–639.
5. Gopalan A, Sharp DS, Fine SW, *et al*. Urachal carcinoma: a clinicopathologic analysis of 24 cases with outcome correlation. *Am J Surg Pathol*, 2009, 33: 659–668.
6. Sheldon CA, Clayman RV, Gonzalez R, *et al*. Malignant urachal lesions. *J Urol*, 1984, 131: 1–8.
7. Mostofi FK, Thomson RV, Dean AL Jr. Mucous adenocarcinoma of the urinary bladder. *Cancer*, 1955, 8: 741–758.
8. Szarvas T, Módos O, Niedworok C, *et al*. Clinical, prognostic, and therapeutic aspects of urachal carcinoma—A comprehensive review with meta-analysis of 1,010 cases. *Urol Oncol*, 2016, 34: 388–398.
9. Hayashi T, Yuasa T, Uehara S, *et al*. Clinical outcome of urachal cancer in Japanese patients. *Int J Clin Oncol*, 2016, 21: 133–138.
10. Siefker-Radtke AO, Gee J, Shen Y, *et al*. Multimodality management of urachal carcinoma: the M. D. Anderson Cancer Center experience. *J Urol*, 2003, 169: 1295–1298.
11. Williamson SR, Lopez-Beltran A, Montironi R, *et al*. Glandular lesions of the urinary bladder: clinical significance and differential diagnosis. *Histopathology*, 2011, 58: 811–834.
12. Verma A, Tomar V. Signet ring cell carcinoma of urachal origin presenting as irritative lower urinary tract symptoms and pain abdomen: a rare case report. *J Clin Diagn Res*, 2016, 10: PD12–PD13.
13. Chen ZF, Wang F, Qin ZK, *et al*. Clinical analysis of 14 cases of urachal carcinoma. *Chines J Cancer (Chinese)*, 2008, 27: 966–969.
14. Vipulkumar Dadhania, Bogdan Czerniak, Charles C Guo. Adenocarcinoma of the urinary bladder. *Am J Clin Exp Urol*, 2015, 3: 51–63.
15. Bruins HM, Visser O, Ploeg M, *et al*. The clinical epidemiology of urachal carcinoma: results of a large, population based study. *J Urol*, 2012, 188:1102–1107.
16. Behrendt MA, DE Jong J, VANR hijn BW. Urachal cancer: contemporary review of the pathological, surgical, and prognostic aspects of this rare disease. *Minerva Urol Nefro*, 2016, 68: 172–184.

DOI 10.1007/s10330-017-0246-6

Cite this article as: Liu KH, Wang HQ, Yu L, *et al*. Primary urachal adenocarcinoma: a rare case report. *Oncol Transl Med*, 2017, 3: 267–269.

Oncology and Translational Medicine

Aims & Scope

Oncology and Translational Medicine is an international professional academic periodical. The Journal is designed to report progress in research and the latest findings in domestic and international oncology and translational medicine, to facilitate international academic exchanges, and to promote research in oncology and translational medicine as well as levels of service in clinical practice. The entire journal is published in English for a domestic and international readership.

Copyright

Submission of a manuscript implies: that the work described has not been published before (except in form of an abstract or as part of a published lecture, review or thesis); that it is not under consideration for publication elsewhere; that its publication has been approved by all co-authors, if any, as well as – tacitly or explicitly – by the responsible authorities at the institution where the work was carried out.

The author warrants that his/her contribution is original and that he/she has full power to make this grant. The author signs for and accepts responsibility for releasing this material on behalf of any and all co-authors. Transfer of copyright to Huazhong University of Science and Technology becomes effective if and when the article is accepted for publication. After submission of the Copyright Transfer Statement signed by the corresponding author, changes of authorship or in the order of the authors listed will not be accepted by Huazhong University of Science and Technology. The copyright covers

the exclusive right and license (for U.S. government employees: to the extent transferable) to reproduce, publish, distribute and archive the article in all forms and media of expression now known or developed in the future, including reprints, translations, photographic reproductions, microform, electronic form (offline, online) or any other reproductions of similar nature.

Supervised by

Ministry of Education of the People's Republic of China.

Administered by

Tongji Medical College, Huazhong University of Science and Technology.

Submission information

Manuscripts should be submitted to:
<http://otm.tjh.com.cn>
dmedizin@sina.com

Subscription information

ISSN edition: 2095-9621
CN: 42-1865/R

■ Subscription rates

Subscription may begin at any time. Remittances made by check, draft or express money order should be made payable to this journal. The price for 2017 is as follows: US \$ 30 per issue; RMB ¥ 28.00 per issue.

Database

Oncology and Translational Medicine is abstracted and indexed in EM-BASE, Index Copernicus, Chinese Science and Technology Paper Citation Database (CSTPCD), Chinese Core Journals Database, Chinese Journal Full-text Database (CJFD), Wanfang

Data; Weipu Data; Chinese Academic Journal Comprehensive Evaluation Database.

Business correspondence

All matters relating to orders, subscriptions, back issues, offprints, advertisement booking and general enquiries should be addressed to the editorial office.

Mailing address

Editorial office of
Oncology and Translational Medicine
Tongji Hospital
Tongji Medical College
Huazhong University of Science and Technology
Jie Fang Da Dao 1095
430030 Wuhan, China
Tel.: +86-27-83662630
Fax: +86-27-83662645
Email: dmedizin@tjh.tjmu.edu.cn

Printer

Changjiang Spatial Information Technology Engineering Co., Ltd. (Wuhan)
Hangce Information Cartography Printing Filial, Wuhan, China
Printed in People's Republic of China

Managing director

Jun Xia

Executive editors

Jing Chen
Jun Xia
Yening Wang
Qiang Wu